DESIGN A SOLAR HYBRID AIR CONDITIONING COMPRESSOR SYSTEM

by

Thomas Chin Jun Yen

14982

Dissertation submitted in partial fulfilment of

the requirements for the

Bachelor of Engineering (Hons)

(Mechanical)

JANUARY 2015

Universiti Teknologi PETRONAS
Bandar Seri Iskandar
31750 Tronoh
Perak Darul Ridzuan

CERTIFICATION OF APPROVAL

Design a Solar Hybrid Air Conditioning Compressor System

by

Thomas Chin Jun Yen
14982

A project dissertation submitted to the
Mechanical Engineering Programme
Universiti Teknologi PETRONAS
in partial fulfilment of the requirement for the
BACHELOR OF ENGINEERING (Hons)
(MECHANICAL)

Approved by,

_____
(Dr. Morteza Khalaji Assadi)

UNIVERSITI TEKNOLOGI PETRONAS
TRONOH, PERAK
January 2015

CERTIFICATION OF ORIGINALITY

This is to certify that I am responsible for the work submitted in this project, that the original work is my own except as specified in the references and acknowledgements, and that the original work contained herein have not been undertaken or done by unspecified sources or persons.

_____

THOMAS CHIN JUN YEN

ABSTRACT

This thesis presents the investigation into the feasibility of solar assisted vapour compression air conditioning system in providing thermal comfort in Malaysia. Conventional vapour compression air conditioning system consumes large amount of energy which is a clear disadvantage considering the high fuel price and electric tariff. Therefore, this research was intended to develop and integrate solar hybrid system into conventional air conditioning system which provides the same cooling load with considerably less electricity demand. In addition, Microsoft Excel spreadsheet is also prepared to facilitate the calculation of refrigerant temperature and energy saving of the system. DC compressor and evacuated tube solar compressor is introduced to assist the electric compressor in compressing the refrigerant, effectively reducing the air conditioning electricity consumption by up to 45%. Meanwhile, during night time, energy saving is only contributed by the DC compressor which reduces electricity consumption by up to 25%. The development and utilization of solar energy reduces the dependency on energy generation from fossil fuel which emits greenhouse gases and worsen the global warming while also pushing Malaysia one step closer to their aim in reducing CO_2 emissions and harnessing renewable energy. Malaysia as a tropical country with average solar radiation of 4500Wh/m² per day, has endless potential in solar energy (Borhanazad, 2013). This project provides technical overview which involves the study of solar energy conversion system and viability of solar hybrid vapour compression air conditioning system under Malaysia climate.

ACKNOWLEDGEMENTS

In completing my Final Year Project, it is sufficed to say that it has taught me valuable insights from the difficulties and struggles that I have encountered. With that, I would like express my heartiest gratitude to all relevant personnel that has assisted me throughout the project.

First and foremost, I would like to express my gratitude towards my supervisor, Dr. Morteza Khalaji Assadi who has been the thrust of this entire project. Your lessons and aid have surely provided me with a clear guidance and understanding along the way. Besides that, I would like to thank my examiner, Dr. Syed Ihtsham Ul Haq Gilani for his critical comments and evaluations given during the completion of this study. I would not be able to complete the study without their assistance and warm hospitality.

I would also like to extend my appreciation to all my family members, especially my father, Chin Wui Hon and mother, Chong Kiaw Lan for being very supportive and caring all the time.

Last of all, thanks to all my friends for all the support and encouragement that has enlightened me to succeed brilliantly in my study. All of the contribution, knowledge and experience are very much appreciated. Above all, such special traits as these can hardly be gained elsewhere, and shall be treasured and used as guidance in the complexity of work, society and corporate life near future.

TABLE OF CONTENTS

LIST OF FIGURES

LIST OF TABLES

ABBREVIATIONS AND NOMENCLATURES

AC – Alternating Current

BLDC – Brushless Direct Current

CO_2 – Carbon Dioxide

COP – Coefficient of Performance

DC – Direct Current

FYP – Final Year Project

P – Pressure

RM – Ringgit Malaysia

SEDEX – Science and Engineering Design Exhibition

T – Temperature

TNB – Tenaga National Berhad

UTP – Universiti Teknologi Petronas

V – Volume

CHAPTER 1

INTRODUCTION

1.1 BACKGROUND

The demand of air conditioning has greatly increased since the last decade due to the effect of climate change and global warming. For instance, two-thirds of residents in Malaysia have air conditioners (Daut, 2013). Ochi (1989) states that air conditioning is defined as the simultaneous processing of temperature, humidity, purification and distribution of air current in compliance with the requirement of space needing air conditioning. Generally, air conditioning is a refrigeration cycle which promotes heat removal.

There are several types of vapour compression air conditioning system, ranges from window unit, portable unit, split unit to central air conditioning unit. Regardless of the types, all systems consists of four basic elements which are compressor, condenser, expansion valve and evaporator coil.

According to Rona (2004), conventional air conditioning system would easily drain half of the building total electricity consumption. This translates to worsen of global warming as current electricity is generated from fossil fuels which emits greenhouse gases.

Harvesting solar energy to run the air conditioning system is a highly feasible technique to replace conventional electricity. As a clean and renewable energy source, the widely available solar energy is expected to produce important part of energy needed by the world.

In this project, the author is to develop an evacuated tube solar collector to be integrated to the conventional air conditioning system to further improve the cooling efficiency.

1.1.1 Malaysia Renewable Energy Target

Malaysia is among the most enthusiastic developing country to promote utilization of renewable energy. Recently, Prime Minister Datuk Seri Najib announced the National Green Technology Policy which focuses on renewable energy sector. Some suitable renewable energy sources for Malaysia are biogas, biomass, solid waste, hydro and solar power. Malaysia is targeting for 4000MW of power generated from renewable energy source by year 2030 as shown is Table 1. However, the targeted capacity were not successfully achieved as of year 2013 with just 190MW of total renewable energy (Malaysia Primary Energy Supply Summary, 2013).

Under the policy, Low Carbon Cities Framework and Assessment System is designed to reduce carbon dioxide emission by up to 40% in year 2020, compared to 2005 (National Renewable Energy Policy & Action Plan, 2008). Renewable energy is one of the key element to push forward Malaysia to achieve developed country target by year 2020.

TABLE 1. Targeted Renewable Energy Capacity in Malaysia (National Renewable Energy Policy & Action Plan, 2008)

Year	Biogas (MW)	Biomass (MW)	Solid Waste (MW)	Small Hydro (MW)	Solar (MW)	Total (MW)
2011	20	110	20	60	9	219
2012	35	150	50	110	20	365
2013	50	200	90	170	33	543
2014	75	260	140	230	48	753
2015	100	330	200	290	65	985
2016	125	410	240	350	84	1209
2017	155	500	280	400	105	1440
2018	185	600	310	440	129	1664
2019	215	700	340	470	157	1882
2020	240	800	360	490	190	2080
2025	350	1190	380	490	455	2865
2030	410	1340	390	490	1370	4000

1.1.2 Potential of Solar Energy in Malaysia

- Malaysia is a tropical country located at Earth equator
- The sunshine per day is approximately 12 hours.
- Average Solar Radiation: 14–22 MJ/m² per day

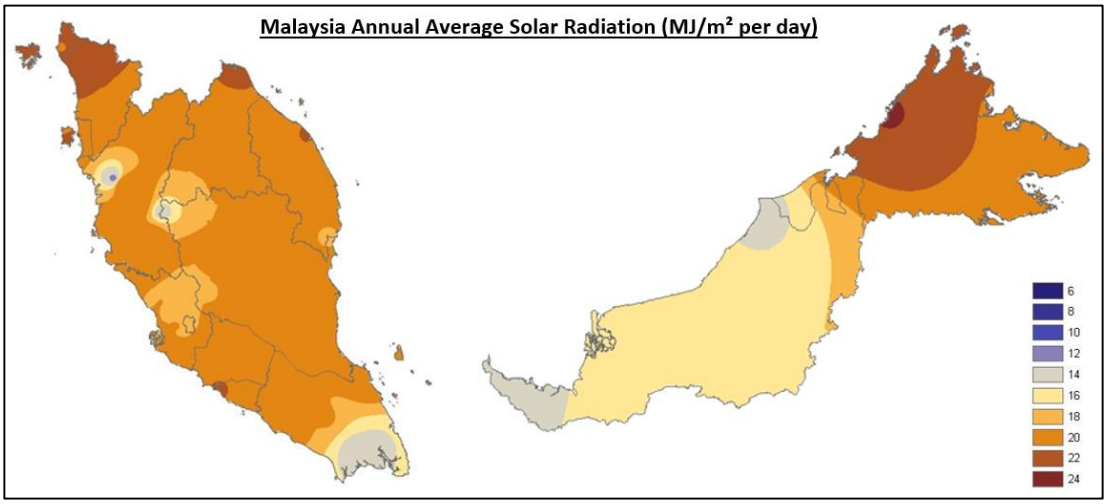

FIGURE 1. Malaysia Annual Average Daily Solar Radiation (MJ/m² per day) (Borhanazad, 2013)

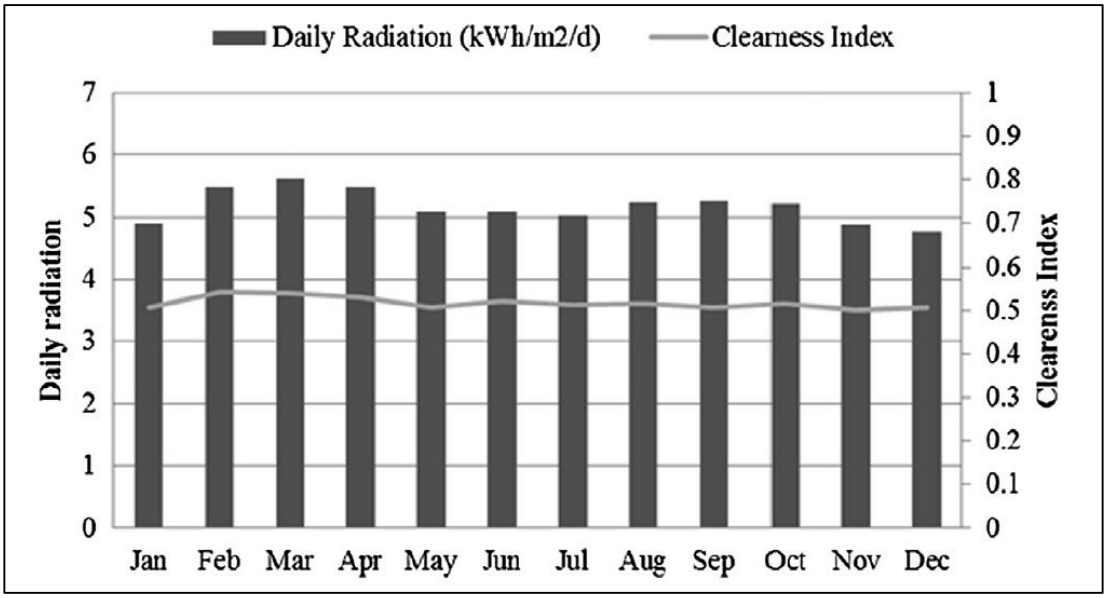

FIGURE 2. Malaysia Monthly Average Daily Solar Radiation (kWh/m² per day) (Borhanazad, 2013)

1.2 Problem Statement

1. High fuel price and electric tariff makes conventional air conditioner not economical in the long run
2. Generating electricity from fossil fuel emits greenhouse gases and worsen the global warming
3. Fossil fuel source is depleting

1.3 Objectives

1. To design and integrate solar hybrid system into conventional air conditioning system
2. To reduce air conditioning electricity consumption by up to 45%
3. To reduce electric peak load during the day

1.4 Scope of Study

1. Understanding the principle of solar energy conversion systems.
2. Understanding the techniques to harvest solar power to improve the conventional air conditioning system.

CHAPTER 2

LITERATURE REVIEW

2.1 Solar Hybrid Air Conditioning Compressor System

Solar hybrid air conditioning system operates the same way as conventional system with one component added, evacuated tube solar collector.

The evacuated tube solar collector is installed between the compressor and condenser. The solar collector consists of high efficient vacuum tube which provides part of compression pressure and heating by further superheating the refrigerant. The higher pressure and larger temperature difference enhance the condensation process in the condenser, resulting in high pressure liquid refrigerant. This configuration greatly reduces energy consumption by reducing the load on electric compressor (Daut, 2013).

Furthermore, the alternating current (AC) compressor is replaced with high efficiency direct current (DC) compressor which consumes considerably less energy at the same load compared to AC compressor (Henning, 2007). DC compressor is powered by high torque brushless motor which is smaller in size and able to operate at variable speed.

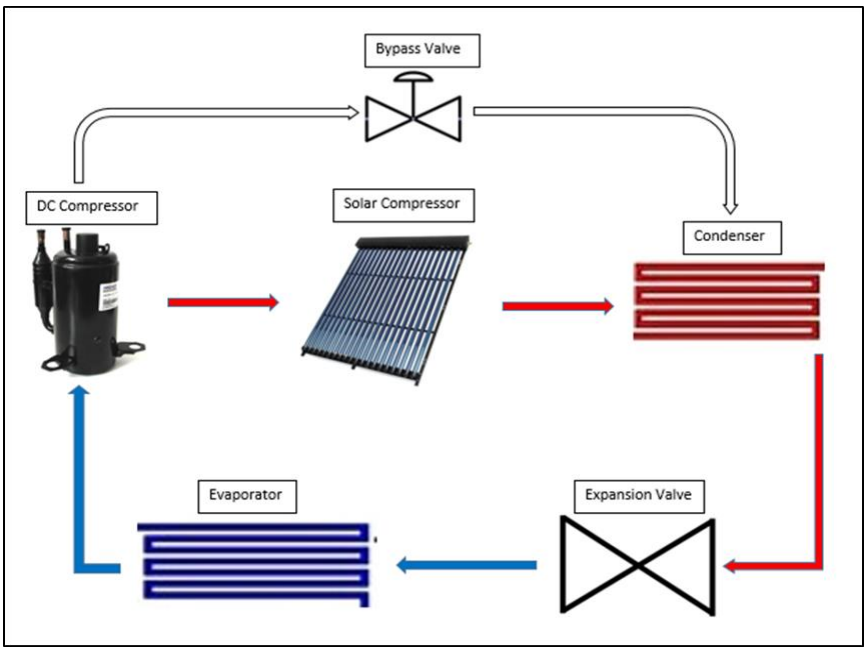

FIGURE 3. Solar Air Conditioning System (Kalkan, 2011)

2.2 Refrigeration Cycle

During refrigeration process, the refrigerant experiences huge change in thermodynamic properties and involves heat energy transfer to the surroundings through the heat exchangers (Admiraal, 1993). During the operation of a vapor compression refrigeration system, the following processes occurs:

Process 1-2s: Compression

A reversible, adiabatic (isentropic) compression of the refrigerant. The saturated vapour at state 1 is superheated to state 2.

$w_c = h_{2s} - h_1$

Process 2s-3: Condensation

An internally, reversible, constant pressure heat rejection in which the refrigerant is de-superheated and then condensed to a saturated liquid at 3.

$q_h = h_{2s} - h_3$

Process 3-4: Throttling and expansion

An irreversible throttling process in which the temperature and pressure decrease at constant enthalpy.

$h_3 = h_4$

Process 4-1: Evaporation

An internally, reversible, constant pressure heat interaction in which the refrigerant is evaporated to a saturated vapour at state point 1. The latent enthalpy necessary for evaporation is supplied by the refrigerated space surrounding the evaporator. The amount of heat transferred to the working fluid in the evaporator is called the refrigeration load.

$q_L = h_1 - h_4$

The thermal efficiency of the cycle can be calculated as:

$$\eta = \frac{q_{evap}}{w_{comp}} = \frac{h_1 - h_4}{h_{2s} - h_1}$$

2.3 Pressure-Enthalpy Diagram

The pressure-enthalpy, P-h diagram is deemed as most important graphical tool in any refrigeration analysis. For instance, two pressure region is involved in a single stage refrigeration cycle, namely high and low pressure region. The P-h diagram clearly illustrates any changes in pressure and enthalpy of the refrigerant which are the key elements in calculation and analysis of performance, heat and work transfer of the refrigeration cycle (Demma, 2005).

On the P-h diagram, the x-axis shows the enthalpy, h (kJ/kg), while the y-axis displays the pressure, P (kPa). The y-axis pressure, P is plotted in logarithmic scale. The two-phase region is separated from the subcooled liquid and superheated vapour region by the 'bell' curve which is jointly formed by the saturated liquid and vapour line. Within the two-phase region, the dryness fraction determines the properties of the refrigerant.

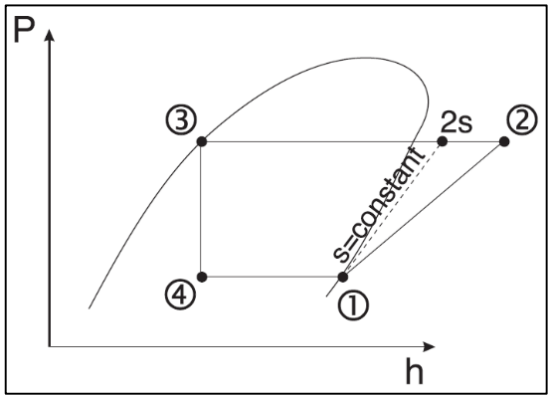

FIGURE 4. P-h diagram of vapour compression refrigeration cycle (Demma, 2005)

2.4 Temperature-Entropy Diagram

The temperature-entropy, T-s diagram is useful in evaluating the isentropic efficiency of the refrigeration cycle. For instance, the T-s diagram is able to clearly show the actual and ideal entropy of refrigerant after passing through the compressor, which is needed to determine the compressor isentropic efficiency (Demma, 2005). The analysis of irreversibilities helps to determine the optimum operating parameters to improve the refrigeration system performance. On the T-s diagram, the x-axis shows the entropy, h (kJ/kg-K), while the y-axis displays the temperature, T (K).

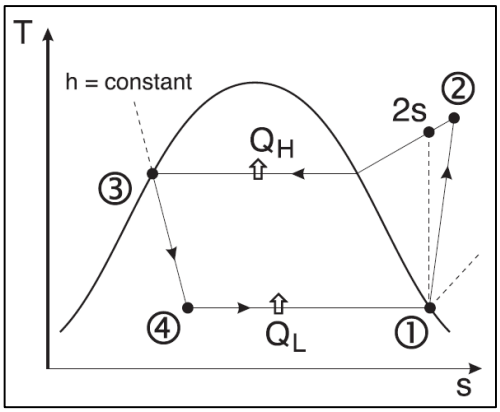

FIGURE 5. T-s diagram of vapour compression refrigeration cycle (Demma, 2005)

2.5 Evacuated Tube Solar Collector

Evacuated tube solar collectors consists of series of glass tubes which has the air evacuated out, creating a vacuum between the glass tube surface and absorber surface. The vacuum layer eliminates heat loss through conduction and convection, leaving radiation as the only heat loss mechanism (Jafarkazemi, 2012). The lower heat loss contributes to more absorbed heat energy, which translates to higher overall efficiency of the solar collector. Furthermore, the cylindrical shape of each evacuated tube allows the solar collector to passively track the sun throughout the day (Karim, 2014). For instance, an evacuated facing south will have the sunlight always striking at right angle to the cylindrical surface. This design provides advantage in term of maximum exposed solar radiation and also reduced reflection. In addition to the vacuum, special absorbing film with high absorptivity is used to absorb up to 90-92% of the sun's ultraviolet rays (Budihardjo, 2008).

The solar collector provides part of compression pressure by heating the refrigerant under constant volume. Ideal gas law states that $PV=nRT$, where P is absolute pressure of gas, V is volume of gas, n is number of moles of gas, R is ideal gas constant, and T is absolute temperature of gas. During the 2nd stage compression, V, n, and R are kept constant, deriving the ideal gas law into $\frac{P_1}{T_1} = \frac{P_2}{T_2}$, where P_1 is the input pressure, T_1 is input temperature, P_2 is the output pressure, and T_2 is output temperature. Therefore, the higher the temperature of solar collector, the higher the pressure of refrigerant.

Heat loss coefficient:

(i) Radiation coefficient between the copper tube and the glass cover:

$$h_{r,t-c} = \frac{\sigma(T_t^2 + T_c^2)(T_t + T_c)}{\frac{1}{\varepsilon_t} + \frac{1}{\varepsilon_c} - 1}$$

(ii) Radiation coefficient for the glass cover to the air:

$$h_{r,c-a} = \varepsilon_c \sigma(T_c^2 + T_s^2)(T_c + T_s)$$

(iii) Convection coefficient for the glass cover to the air:

$$h_{c,c-a} = \frac{k}{D_c} Nu$$

$$Rayleigh\ number, Ra = \frac{g\beta(T_c - T_a)D_c^3}{\upsilon^2} Pr$$

$$Nusselt\ number, Nu = \left[0.6 + \frac{0.387Ra^{\frac{1}{6}}}{\left[1 + \left(\frac{0.559}{Pr}\right)^{\frac{9}{16}}\right]^{\frac{8}{27}}}\right]^2$$

(iv) Top loss coefficient:

$$U = \left(\frac{1}{(A_t)(h_{r,t-c})} + \frac{1}{(A_c)(h_{r,c-a} + h_{c,c-a})}\right)^{-1}$$

(v) Glass cover temperature

$$T_c = T_t - \frac{U\left[\frac{h_{r,c-a}}{h_{r,c-a} + h_{c,c-a}}(T_t - T_s) + \frac{h_{c,c-a}}{h_{r,c-a} + h_{c,c-a}}(T_t - T_a)\right]}{(A_t)h_{r,t-c}}$$

Rate of energy balance equation:

$$h_{r,t-c} = h_{r,c-a} + h_{c,c-a}$$

$$\frac{\sigma A_t(T_t^4 - T_c^4)}{\frac{1}{\varepsilon_t} + \frac{1 - \varepsilon_c}{\varepsilon_c}\left(\frac{D_t}{D_c}\right)} = \varepsilon_c \sigma A_c(T_c^4 - T_s^4) + h_{c,c-a}A_c(T_c - T_a)$$

Where:

ε_t = copper tube emittance

ε_c = glass cover emittance

T_a = ambient temperature (K)

T_s = sky temperature (K)

T_t = mean tube temperature (K)

T_c = glass cover temperature (K)

A_t = area of absorber tube, m²

A_c = area of glass cover, m²

σ = Stefan-Boltzman constant ($5.67x10^{-8}W/m^2K^4$)

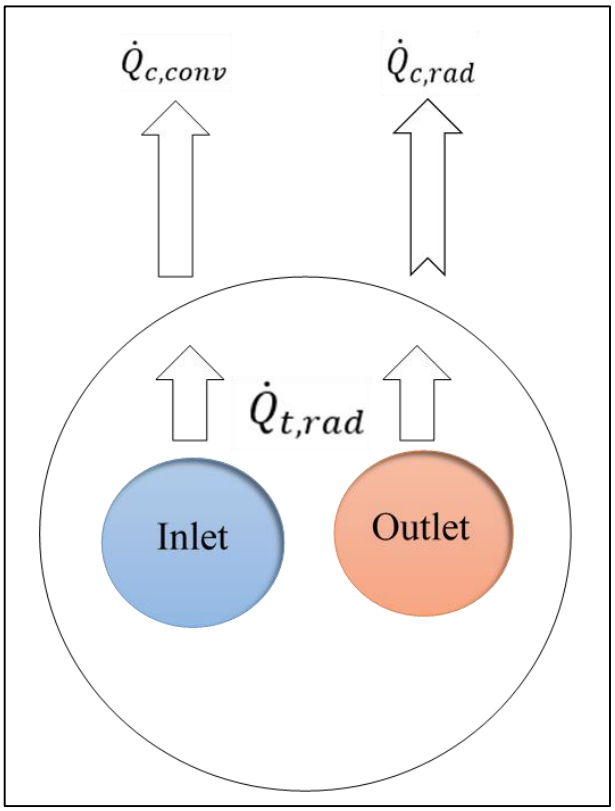

FIGURE 6. Thermal network for U-tube evacuated solar collector

2.6 Type of Evacuated Solar Collector

(i) Heat Pipe Evacuated Solar Collector

Heat pipe solar collector has a metal heat pipe, attached to selective absorber plate in the evacuated tube. The heat pipe contain a small quantity of liquid, such as alcohol, acetone or purified water plus special additives. Inside, the heat pipe is evacuated which lowers the boiling point of the working fluid, enabling the system to start working even at low temperatures (Kalogirou, 2014). When solar radiation strikes the collector, the working liquid quickly evaporate and rises to the copper header. The refrigerant flows through a manifold and absorb the heat from the copper header, causing the working fluid to condense and flow back down to the heat tube where the heat exchange process is repeated.

Since there is no direct connection between the evacuated tubes with the flowing refrigerant, the system is still functional despite one broken tube. Moreover, installation process is easier where individual tube can be replaced without shutting down the system or emptying the refrigerant. However, heat pipe solar collector must be mounted at a minimum tilt angle of 25° as the condensed working fluid rely on gravitational pull to return to the absorber area (Ong, 2012).

(ii) U-tube Evacuated Solar Collector

U-tube collector consists of long copper tube which directs the refrigerant flow through the evacuated tube (Kalogirou, 2014). This allows a greater heat exchanging area which is highly desirable due to the low thermal conductivity of refrigerant vapour. The copper tube has fin which is covered with special coating to maximise absorption of solar radiation. The radiation and convection heat loss is effectively prevented by the evacuated tube.

U-tube collector is better than the heat pipe in terms of initial cost and smaller sizing. Moreover, U-tube collector has less constrain on installation position where it can be mounted perfectly horizontal or vertical (Ong, 2012). However, U-tube collector falls behind in terms of maintenance and reliability. Since the refrigerant is flowing through the evacuated tube, a broken tube will affect the whole system and changing tubes will require the refrigerant to be emptied.

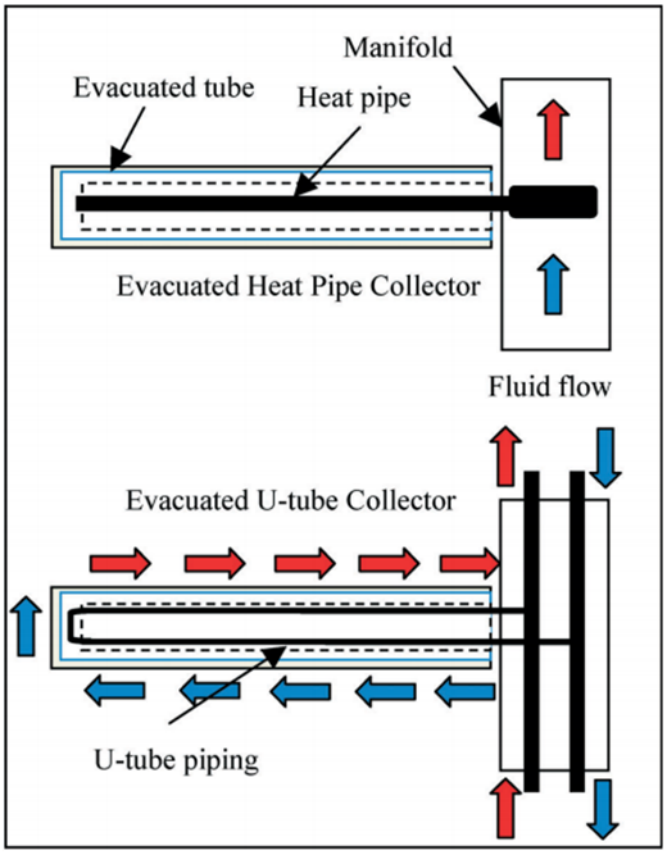

FIGURE 7. Heat Pipe and U-tube evacuated solar collector (Ong, 2012)

2.7 Direct Current (DC) Compressor

Direct current (DC) compressor has become more popular due to its advantages over the conventional alternating current (AC) compressor in air conditioning system (Kohlenbach, 2014). Conventional AC compressor utilises 3-phase AC induction motor due to the simple design, low initial cost and high reliability. However, it is difficult to control the speed of AC motor so most air conditioning systems are using single speed AC compressor (Brown, 2007). Therefore, the air conditioning system needs to constantly switch on and off the compressor to maintain the desired temperature which leads to high energy consumption and noisy operation. While AC inverter motor enable the compressor to work at variable speed, the AC inverter system is expensive and have lower efficiency compared to DC brushless motor.

DC compressor uses brushless dc (BLDC) motor which has relatively flat speed-torque output and high power to size ratio. Therefore, BLDC motor are able to operate at variable speed without compromising torque which allows the system to dynamically adjust its capacity based on cooling requirement. The variable speed operation ensures

continue delivery of cool air which contributes to less temperature fluctuation and more comfortable environment for the occupant (Brown, 2007). Furthermore, while BLDC motor has permanent magnets on rotor and no brushes for commutation, the motor is highly efficient and reliable. However, BLDC motor is has higher initial cost than the simpler AC motor. Nevertheless, the DC compressor are more economical in the long run due to their energy saving capability (Lamanna, 2010).

Figure 8 displays the performance comparison chart among conventional on-off AC compressor, AC inverter compressor, and DC brushless compressor. The comparison chart shows that DC brushless compressor has the highest efficiency over the entire load range.

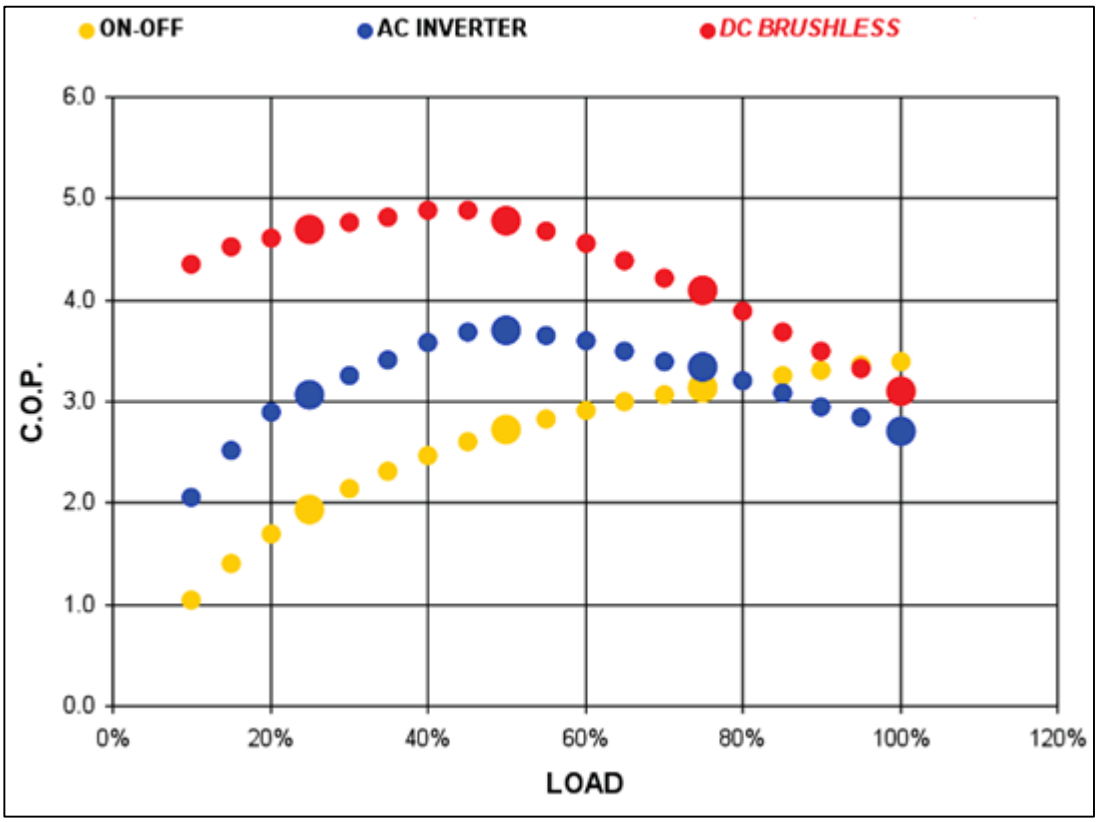

FIGURE 8. Air conditioning compressor performance comparison chart (Lamanna, 2010)

CHAPTER 3

METHODOLOGY

3.1 Research Methodology

In this project, five York Cooling King L Series conventional air conditioner model with capacity ranging from 10000btu/h to 24000btu/h are selected for analysis.

TABLE 2. York Cooling King L Series (York Air Conditioner Brochure, 2014)

Model	**1**	**2**	**3**	**4**	**5**
Cooling Capacity (Btu/h)	10000	13000	18000	19500	24000
Power (W)	815	1015	1360	1540	2230
Current (A)	4.38	5.36	7.16	8.12	12
Compressor Power (W)	735.0	915.0	1222.5	1387.5	2006.3
Refrigerant	R22	R22	R22	R22	R22
COP	3.99	4.16	4.31	4.12	3.51

ANSYS software is used extensively to determine the required length of evacuated tube solar collector and refrigerant output temperature at different hours in a day. The results are then compared with theoretical calculations to determine the energy saving performance. Meanwhile, the results are compared with experiment of other researchers using actual air conditioner and evacuated tube solar collector to further verify the results. In addition, Microsoft Excel spreadsheet is also prepared to facilitate the calculation of refrigerant temperature and energy saving of the system.

Figure 9 below shows the overall progress of the methodology flow in order to conduct Final Year Project (FYP) smoothly and efficiently.

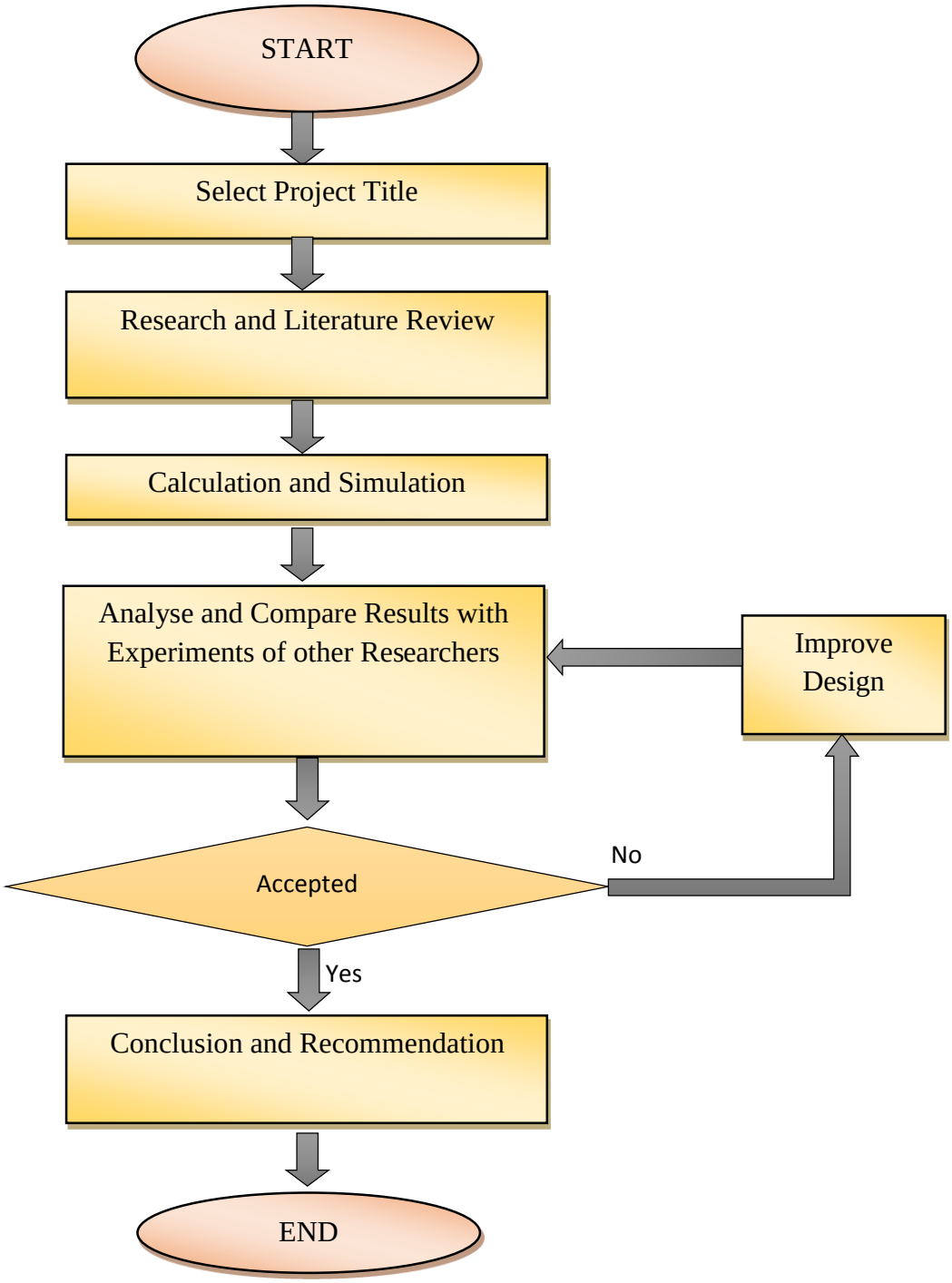

FIGURE 9. Methodology Flow

3.2 Gantt Chart

TABLE 3. Final Year Project (FYP) Gantt Chart

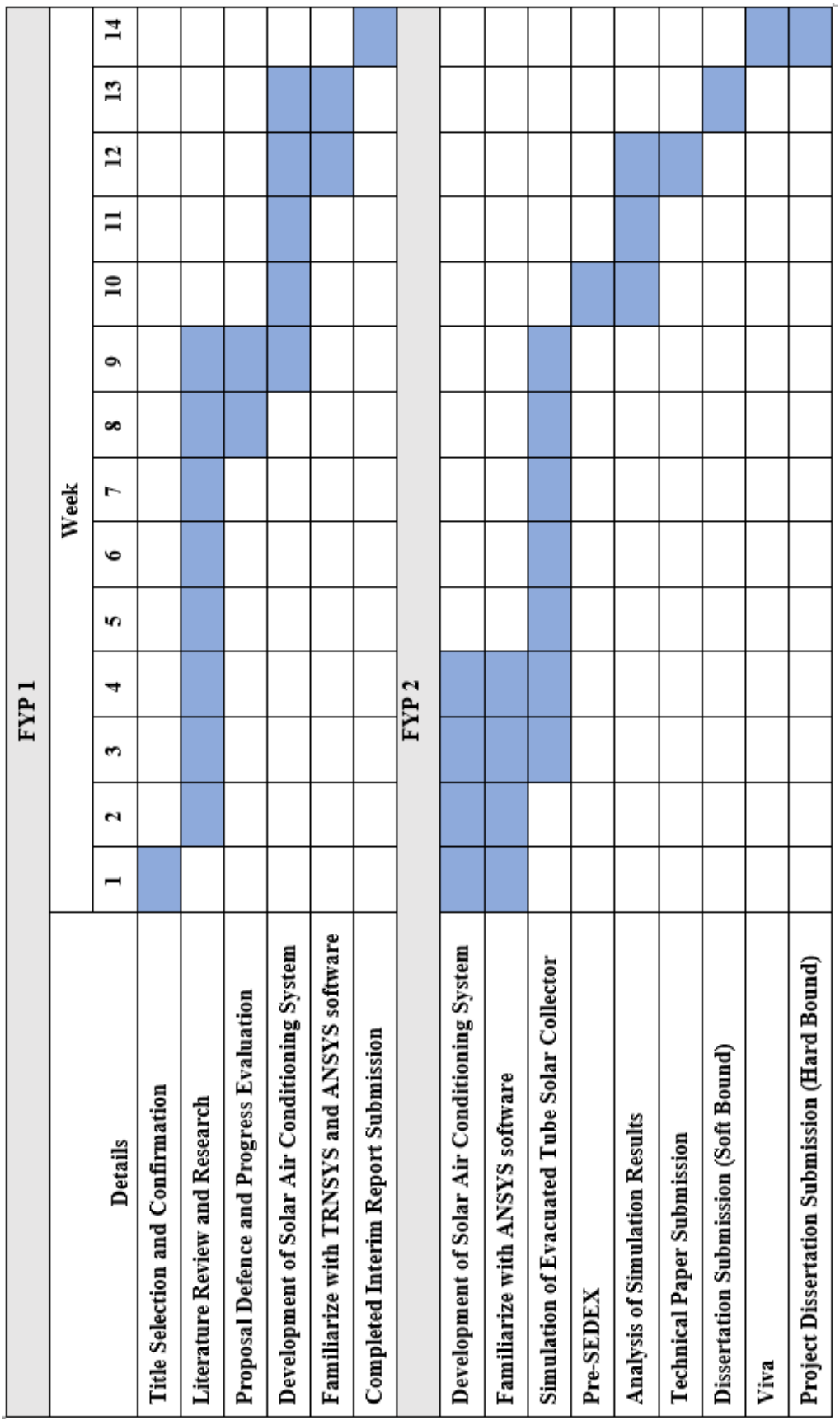

3.3 Key Project Milestone

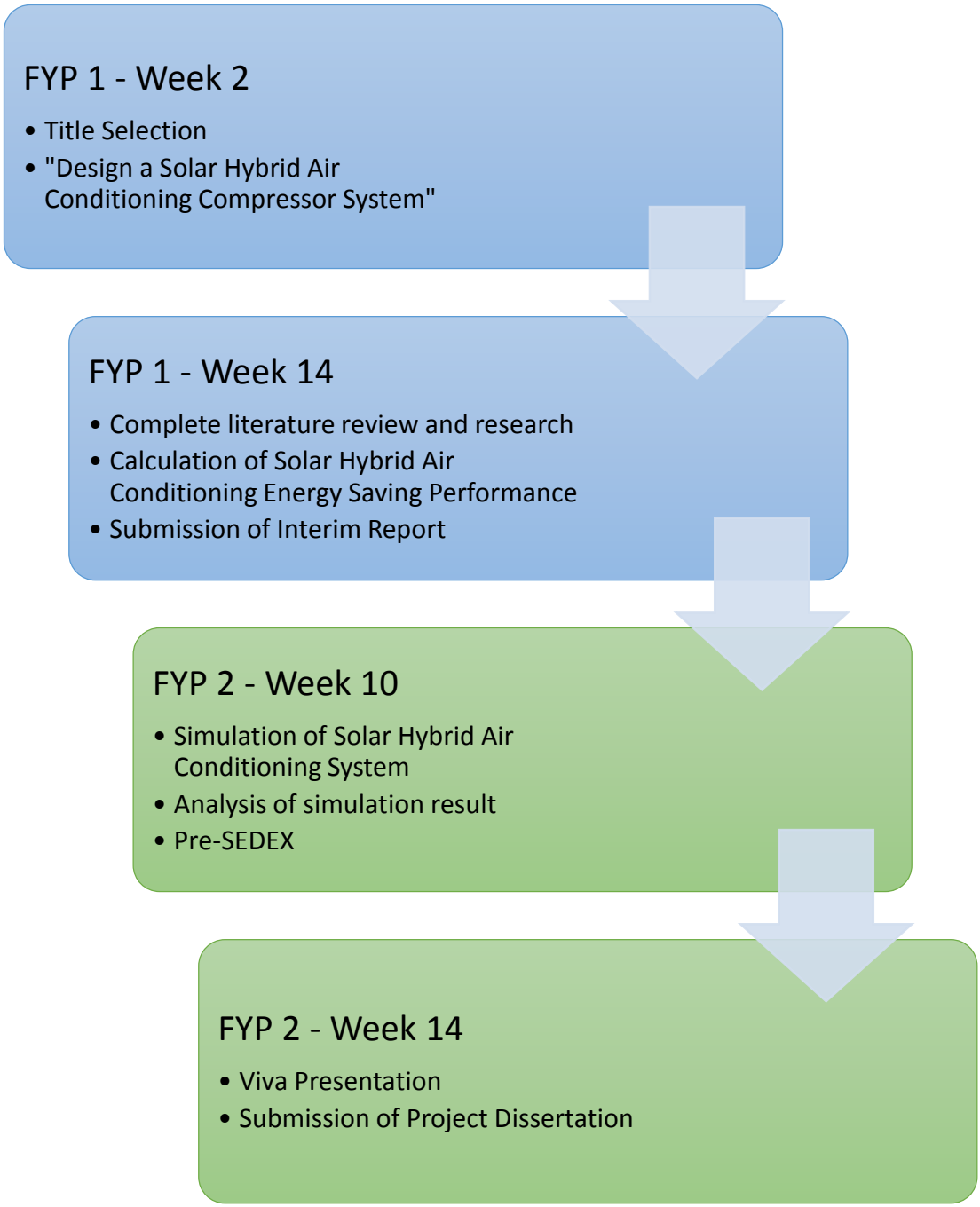

FIGURE 10. Final Year Project (FYP) Project Key Milestone

CHAPTER 4

RESULTS AND DISCUSSIONS

4.1 Refrigeration Cycle Parameter

The conventional air conditioning system uses R22 as the refrigerant and operates on an ideal vapour compression refrigeration cycle between 550kPa and 1700kPa. The ideal refrigeration cycle parameter using R22 refrigerant is shown in the table below:

TABLE 4. Ideal Refrigeration Cycle Parameter

State	**1**	**2**	**3**	**4**
Pressure, P (kPa)	550	1700	1700	550
Temperature, T (°C)	10.00	69.20	40.00	3.09
Enthalpy, h (kJ/kg)	411.3	440.9	249.6	249.6
Entropy, s (kJ/K-kg)	1.765	1.765	1.166	1.180
Quality	Superheated vapour	Superheated vapour	Subcooled liquid	0.227
COP	$COP = \frac{h_1 - h_4}{h_2 - h_1} = \frac{411.3 - 249.6}{440.9 - 411.3} = 5.46$			

An actual vapour compression refrigeration cycle differs from the ideal one in several ways. In the ideal cycle, the refrigerant leaves the evaporator and enters the compressor as saturated vapour. In practice, however, it may not be possible to control the state of the refrigerant so precisely. Instead, it is easier to design the system so that the refrigerant is slightly superheated at the compressor inlet. This slight overdesign ensures that the refrigerant is completely vaporized when it enters the compressor.

Next, in the ideal case, the refrigerant is assumed to leave the condenser as saturated liquid at the compressor exit pressure. In reality, however, it is not easy to execute the condensation process with such precision that the refrigerant is a saturated liquid at the end, and it is undesirable to route the refrigerant to the throttling valve before the refrigerant is completely condensed. Therefore, the refrigerant is subcooled somewhat before it enters the throttling valve (Cengel Y.A. & Boles M. A., 2013).

4.2 Calculation on Air Conditioning Performance

Model 1: (Same calculation method for model 2, 3, 4, and 5)

$$COP = \frac{h_1 - h_4}{h_{2a} - h_1} \rightarrow 3.99 = \frac{411.3 - 249.6}{h_{2a} - 411.3}$$

$$Actual\ Enthalpy, h_{2a} = 451.8\, kJ/kg$$

$$Compressor\ Isentropic\ Efficiency, \eta_c = \frac{h_{2s} - h_1}{h_{2a} - h_1} = \frac{440.9 - 411.3}{451.8 - 411.3} = 0.731$$

$$Compressor\ power = \dot{m}_r(h_{2a} - h_1) \rightarrow 735.0x10^{-3} = \dot{m}_r(451.8 - 411.3)$$

$$Refrigerant\ mass\ flow\ rate, \dot{m}_r = 0.0181\ kg/s$$

Each air conditioner model has different compressor isentropic efficiency and refrigerant mass flow rate. Model 3 has the compressor with highest isentropic efficiency of 78.9%, followed by Model 2, 4 and 1. Model 5 has the lowest compressor isentropic efficiency of 64.2%. Meanwhile, the refrigerant mass flow rate increases with the cooling capacity of air conditioner. Therefore, Model 5 has the highest refrigerant mass flow rate of 0.0435kg/s, followed by Model 4, 3, 2 and 1. The table below shows the compressor isentropic efficiency and refrigerant mass flow rate for each air conditioning model.

TABLE 5. Air conditioning performance comparison

Air Conditioning Model	**1**	**2**	**3**	**4**	**5**
Actual Enthalpy $\boldsymbol{h_{2a}}$ **(kJ/kg)**	451.8	450.2	448.8	450.5	457.4
Compressor Isentropic Efficiency $\boldsymbol{\eta_c = \frac{h_{2s} - h_1}{h_{2a} - h_1}}$	0.731	0.761	0.789	0.755	0.642
Refrigerant mass flow rate $\boldsymbol{\dot{m}_r}$ **(kg/s)**	0.0181	0.0235	0.0326	0.0353	0.0435

4.3 Solar Hybrid Vapour Compression Refrigeration Cycle

The evacuated tube solar collector is installed between the compressor and condenser, providing part of compression pressure and heating by further superheating the refrigerant. Figure 11 and 12 shows the P-h and T-s diagram of solar hybrid vapour compression refrigeration cycle at maximum energy saving where the refrigerant temperature achieved 160°C at the solar collector outlet. The electric DC compressor workload is significantly reduced due to the lower output pressure of 1280kPa compared to the original 1700kPa.

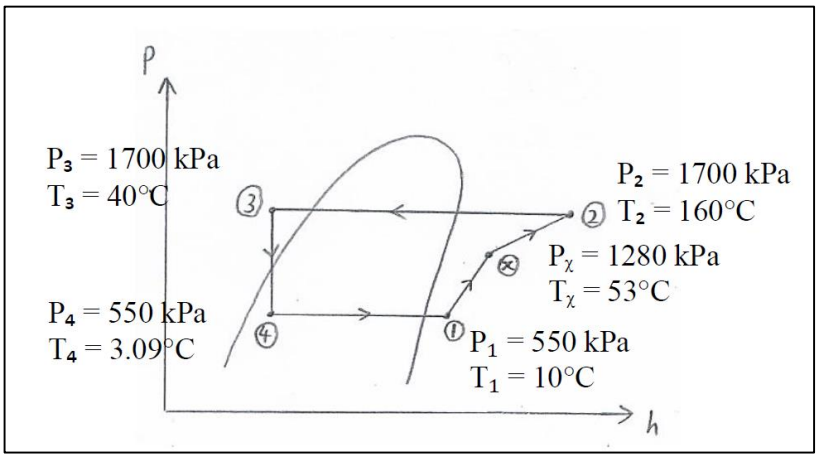

FIGURE 11. P-h diagram of solar hybrid vapour compression refrigeration cycle

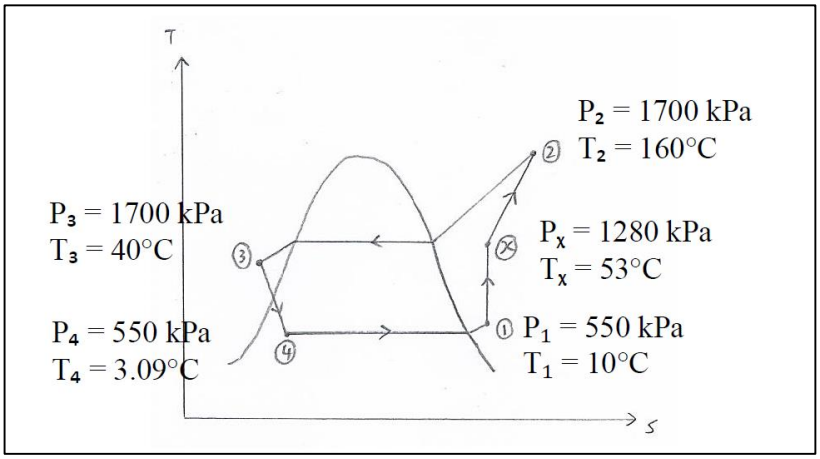

FIGURE 12. T-s diagram of solar hybrid vapour compression refrigeration cycle

Process 1-x: Electric compressor

Process x-2: Solar compressor

Process 2-3: Condenser

Process 3-4: Expansion valve

Process 4-1: Evaporator

4.4 Calculation on Condenser Sizing

Model 1: (Sample Calculation)

Conventional air conditioning system:

$$\dot{Q}_c = \dot{m}_r C_p (T_{out} - T_{in}) = 0.0181(57.2)(69.2 - 40) = 30.23\ W$$

$$T_s = \frac{T_{in} + T_{out}}{2} = \frac{69.2 + 40}{2} = 54.6℃$$

$$\dot{Q}_c = hA_s(T_s - T_a) = h(\pi D L_c)(54.6 - 30) = 30.23\ W \rightarrow ①$$

Solar hybrid air conditioning system:

$$\dot{Q}_s = \dot{m}_r C_p (T_{out} - T_{in}) = 0.0181(57.2)(160 - 40) = 124.24\ W$$

$$T_s = \frac{T_{in} + T_{out}}{2} = \frac{160 + 40}{2} = 100℃$$

$$\dot{Q}_s = hA_s(T_s - T_a) = h(\pi D L_s)(100 - 30) = 124.24\ W \rightarrow ②$$

Comparing ① to ②:

$$\cancel{h}(\cancel{\pi D} L_c)(54.6 - 30) = 30{,}23 \rightarrow \cancel{h}(\cancel{\pi D}) L_c = 1.22$$

$$\cancel{h}(\cancel{\pi D} L_s)(100 - 30) = 124.24 \rightarrow \cancel{h}(\cancel{\pi D}) L_s = 1.77$$

$$\frac{L_s}{L_c} = \frac{1.77}{1.22}$$

$$\therefore L_s = 1.45\ L_c$$

Where:

L_s = Solar hybrid air conditioning system condenser length

L_c = Conventional air conditioning system condenser length

TABLE 6. Solar hybrid air conditioning system condenser length

	Solar hybrid air conditioning system Condenser Length, L_s
Model 1	1.45 L_c
Model 2	1.44 L_c
Model 3	1.44 L_c
Model 4	1.44 L_c
Model 5	1.44 L_c

From Table 6, all the condensers need to be 45% longer, regardless of models, in order to cool down the refrigerant to 40°C from up to 160°C. The extra refrigerant heat is produced by the solar compressor which uses the solar thermal energy to increase the refrigerant pressure. In contrast, the conventional unit only has to cool down the refrigerant temperature from 69.2°C to 40°C. The refrigerant is further subcooled before entering the throttle valve while pressure drop in the extra length of condenser is insignificant and can be neglected (Cengel Y.A. & Boles M. A., 2013).

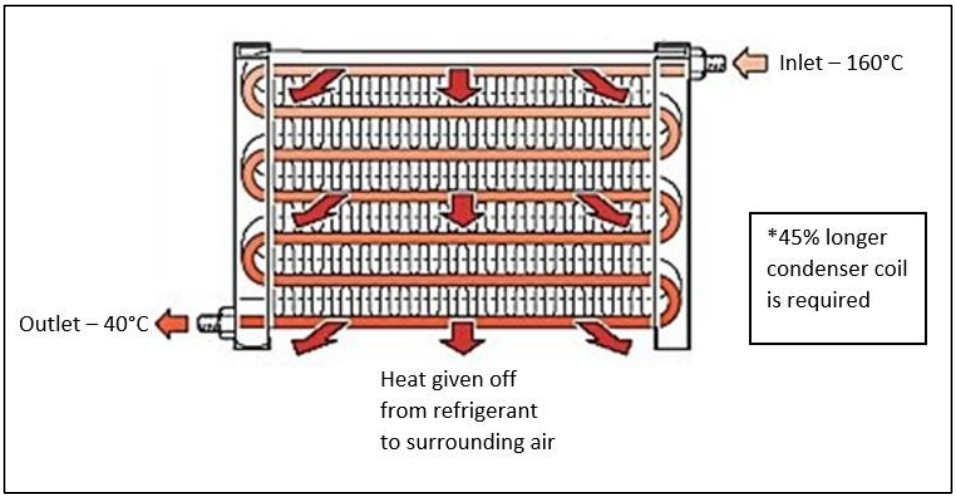

FIGURE 13. Air Conditioner Condenser Coil (TechChoice Part)

4.5 Calculation on Solar Compressor Energy Saving Performance

Set E: P_χ = 1300 kPa; T_χ = 54.1°C; s_χ = 1.765 kJ/kg-K

(Same calculation method for Set A, B, C, D, and F)

(i) Ideal cycle:

h_χ = 432.9 kJ/kg

$$Compressor\ energy\ saving = 1 - \frac{h_x - h_1}{h_2 - h_1}\ x\ 100\%$$

$$= 1 - \frac{432.9 - 411.3}{440.9 - 411.3}\ x\ 100\% = 27\%$$

(ii) Model 1: (Same calculation method for model 2, 3, 4, and 5)

Replace electric compressor to DC compressor with 90% efficiency.

$$\eta_c = \frac{h_{xs} - h_1}{h_{xa} - h_1} \rightarrow 0.90 = \frac{432.9 - 411.3}{h_{xa} - 411.3}$$

$$h_{xa} = 435.3\ kJ/kg$$

$$Compressor\ energy\ saving = 1 - \frac{h_{xa} - h_1}{h_{2a} - h_1}\ x\ 100\%$$

$$= 1 - \frac{435.3 - 411.3}{451.8 - 411.3}\ x\ 100\% = 40.7\%$$

With evacuated tube solar collector, compressor energy saving of 28.6% can be achieved. When combined with high efficiency DC compressor, the solar compressor can achieve energy saving up to 49.4%, depending on the model. Table 7 shows the compressor energy saving performance for all model at different refrigerant temperature at condenser inlet.

TABLE 7. Compressor energy saving performance comparison

Set		**A**	**B**	**C**	**D**	**E**	**F**
Refrigerant Temperature after Solar Compressor, °C		69.2	86.7	106.8	129.2	154.7	160.0
(1) Electric Compressor Inlet	P_1 (kPa)	550	550	550	550	550	550
	T_1 (°C)	10	10	10	10	10	10
	h_1 (kJ/kg)	411.3	411.3	411.3	411.3	411.3	411.3
(x) Solar Compressor Inlet	P_x (kPa)	N/A	1600	1500	1400	1300	1280
	T_x (°C)	N/A	65.7	62.1	58.2	54.1	53.0
	h_{xs} (kJ/kg)	N/A	438.9	436.9	434.9	432.9	432.7
(2) Condenser Inlet	P_2 (kPa)	1700	1700	1700	1700	1700	1700
	T_2 (°C)	69.2	86.7	106.8	129.2	154.7	160.0
Compressor Energy Saving, %							
Ideal		0	6.8	13.5	20.3	27.0	28.6
Model 1		18.8	24.2	29.9	35.3	40.7	41.3
Model 2		15.4	21.2	27.0	32.6	38.3	39.7
Model 3		12.3	18.1	24.3	30.1	36.0	38.1
Model 4		16.1	21.7	27.6	33.2	38.8	40.5
Model 5		28.6	33.4	38.4	43.2	47.9	49.4

The higher the refrigerant temperature, the higher the compressor energy saving, thus contributing to lower power consumption. However, the maximum compressor energy saving is limited at 160°C of refrigerant temperature at condenser inlet. The designated condenser is unable to remove any excess heat energy from the refrigerant at temperature higher than 160°C. In short, the solar compressor provide energy saving when refrigerant temperature at condenser inlet is in the range of 69.2°C up to 160°C. At refrigerant temperature lower than 69.2°C, the energy saving is solely supported by the highly efficient DC compressor. Figure 14 shows the compressor energy saving at different refrigerant temperature.

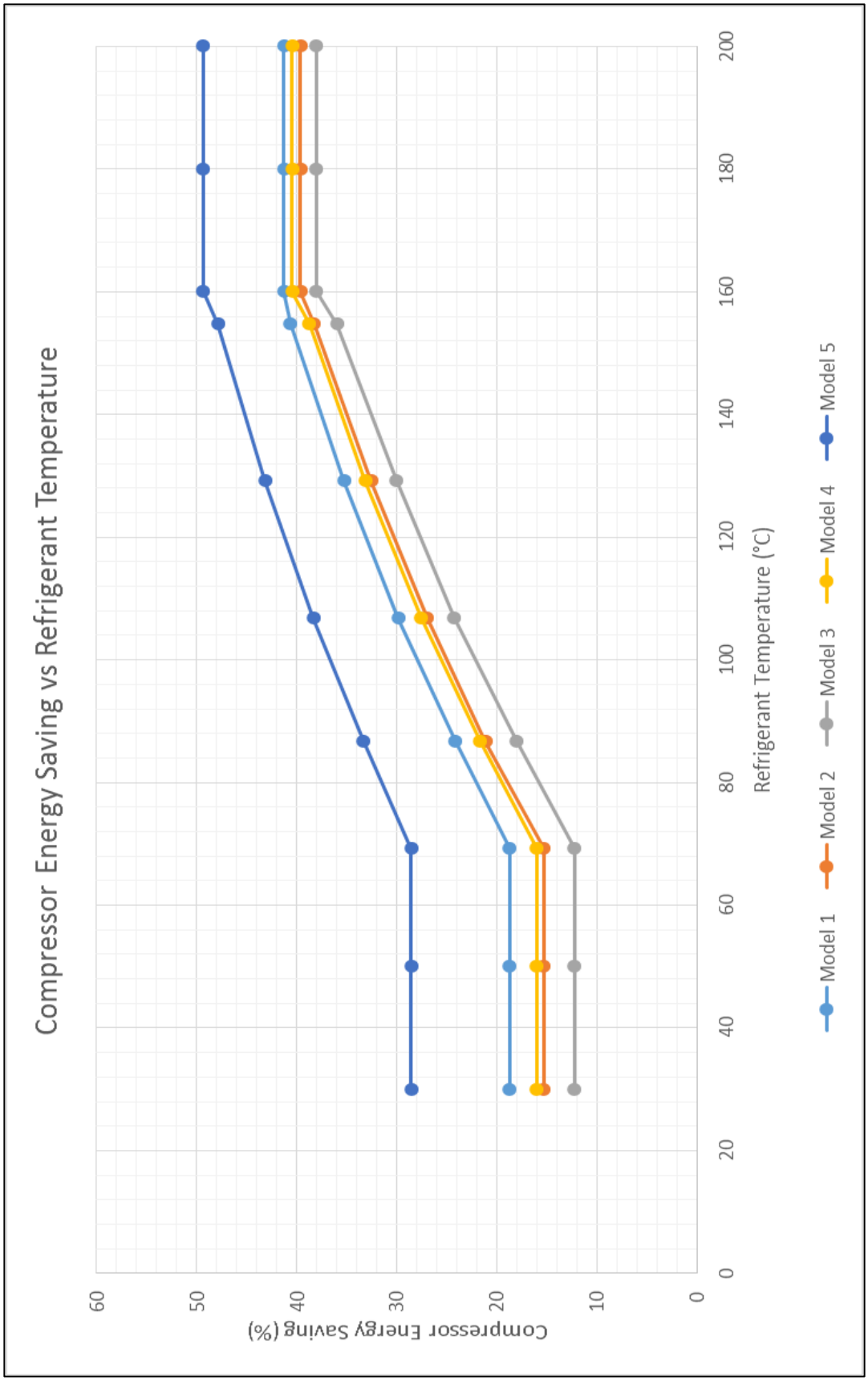

FIGURE 14. Comparison Graph of Compressor Energy Saving vs Refrigerant Temperature at Condenser Inlet

4.6 Solar Hybrid Air Conditioning System Energy Saving Performance

Model 1: (Same calculation method for model 2, 3, 4, and 5)

Conventional air conditioning system power consumption – 815 W

Conventional AC compressor power consumption – 735 W

(i) Solar hybrid air conditioning system energy saving, S

$$S = \frac{(735\ x\ Compressor\ Energy\ Saving)}{815}\ x\ 100\%$$

(ii) Solar hybrid air conditioning system power consumption, P

$$P = 815\ x\ System\ Energy\ Saving$$

The higher the compressor energy saving, the higher the system energy saving, thus contributing to lower power consumption. Table below shows the solar hybrid air conditioning system energy saving and power consumption for all models.

TABLE 8. Solar hybrid air conditioning system energy saving and power consumption

Refrigerant Temperature after Solar Compressor, °C	69.2	86.7	106.8	129.2	154.7	160.0
Solar Hybrid Air Conditioning System Energy Saving, %						
Model 1	17.0	21.8	27.0	31.8	36.7	37.2
Model 2	13.9	19.1	24.3	29.4	34.5	35.8
Model 3	11.1	16.3	21.8	27.1	32.4	34.2
Model 4	14.5	19.6	24.9	29.9	35.0	36.5
Model 5	25.7	30.0	34.5	38.9	43.1	44.4
Solar Hybrid Air Conditioning System Power Consumption, W						
Model 1	676.8	637.1	595.2	555.5	515.9	511.4
Model 2	874.1	821.0	768.0	716.7	664.6	651.7
Model 3	1209.6	1138.7	1062.9	992.0	919.9	894.2
Model 4	1316.6	1238.9	1157.1	1079.4	1001.7	978.1
Model 5	1656.2	1559.9	1459.6	1363.3	1269.0	1238.9

The solar hybrid air conditioning system energy saving comes from the energy saving achieved by compressor unit. The system energy saving is slightly lower than the compressor energy saving due to the energy consumptions of other components such as indoor air blower and electronic control system. There is a strong relationship between energy saving and power consumption where the higher the energy saving, the lower the power consumption, and vice versa. Figure 15 and 16 shows the solar hybrid air conditioning system energy saving and power consumption for all models.

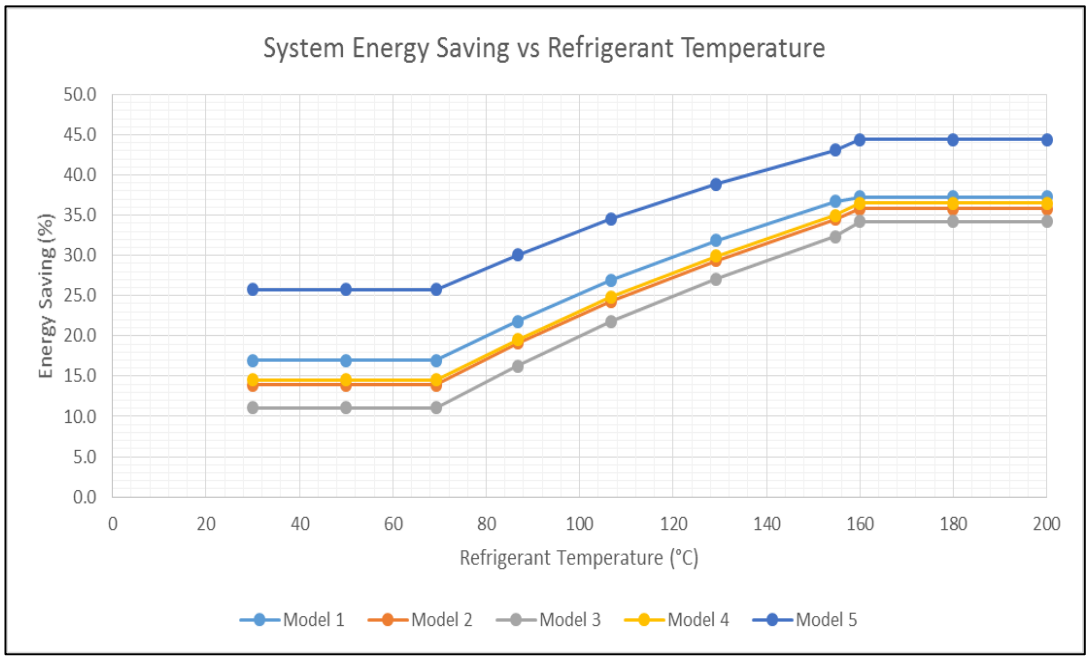

FIGURE 15. Comparison graph of System Energy Saving vs Refrigerant Temperature at Condenser Inlet

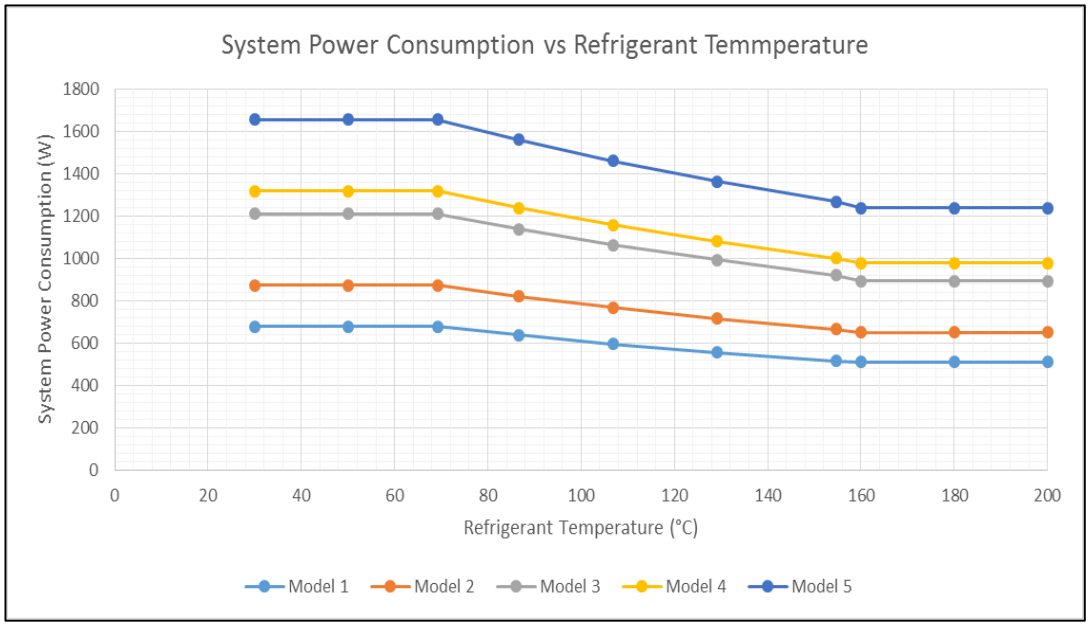

FIGURE 16. Comparison graph of System Power Consumption vs Refrigerant Temperature at Condenser Inlet

4.7 Justification for Evacuated Tube Solar Compressor Position

Set E: (Same calculation method for Set A, B, C, D, and F)

(i) After electric compressor:

Electric Compressor:

Increase pressure from P_1 = 550kPa to P_x = 1300kPa

T_x = 54.1°C ; h_x = 432.9 kJ/kg ; s_x = 1.765 kJ/kg-K

$$h_x - h_1 = 432.9 - 411.3 = 21.6\ kJ/kg$$

Evacuated Tube Solar Compressor:

Increase pressure from P_x = 1300kPa to P_2 = 1700kPa

$$\frac{P_x}{T_x} = \frac{P_2}{T_2} \rightarrow \frac{1300kPa}{327.1K} = \frac{1700kPa}{T_2}$$

$$\therefore\ T_2 = 427.7K = 154.7℃$$

$$Compressor\ energy\ saving = 1 - \frac{h_x - h_1}{h_2 - h_1}\ x\ 100\%$$

$$= 1 - \frac{432.9 - 411.3}{440.9 - 411.3}\ x\ 100\% = 27.0\%$$

In this configuration, the electric compressor needs 27% less energy than the conventional method. Furthermore, T_2 = 154.7°C is achievable by evacuated tube solar collector. Therefore, the evacuated tube solar compressor should be placed after the electric compressor.

(ii) Before electric compressor:

Evacuated Tube Solar Compressor:

Let T_x be 154.7℃

$$\frac{P_1}{T_1} = \frac{P_x}{T_x} \rightarrow \frac{550kPa}{283K} = \frac{P_x}{427.7K}$$

$$\therefore\ P_x = 831.2kPa$$

From the thermodynamic properties table, h_x = 518.9 kJ/kg ; s_x = 2.033 kJ/kg-K

Electric Compressor:

Increase pressure from P_x = 831.2kPa to P_2 = 1700kPa

T_2 = 195°C ; h_2 = 547.9 kJ/kg ; s_2 = 2.033 kJ/kg-K

$h_2 - h_x = 547.9 - 518.9 = 29$ kJ/kg

$$Compressor\ energy\ saving = 1 - \frac{h_{2'} - h_x}{h_2 - h_1}\ x\ 100\%$$

$$= 1 - \frac{547.9 - 518.9}{440.9 - 411.3}\ x\ 100\% = 2.0\%$$

In this configuration, the electric compressor only saves 2.0% energy compared to the conventional method. Furthermore, the high refrigerant temperature of 195°C puts more load on the condenser. Therefore, placing the evacuated tube solar compressor before electric compressor is not desirable.

TABLE 9. Energy saving and refrigerant temperature comparison for different solar compressor position

Set	A	B	C	D	E	F
Evacuated Tube Solar Compressor Placed after Electric Compressor						
Refrigerant Temperature at Condenser Inlet, °C	69.2	86.7	106.8	129.2	154.7	184.2
Compressor Energy Saving, % (Ideal)	0	6.8	13.5	20.3	27.0	33.8
Evacuated Tube Solar Compressor Placed before Electric Compressor						
Refrigerant Temperature at Condenser Inlet, °C	120	134	154	174	195	223
Compressor Energy Saving, % (Ideal)	0	2.0	-5.7	-5.7	2.0	2.0

Both electric compressor and solar compressor uses different ways to pressurise the refrigerant. The electric compressor works by mechanically forcing the refrigerant into a smaller volume while the solar collector provides the compression pressure by heating the refrigerant under constant volume. The study results shown that the solar compressor has to be placed after the electric compressor.

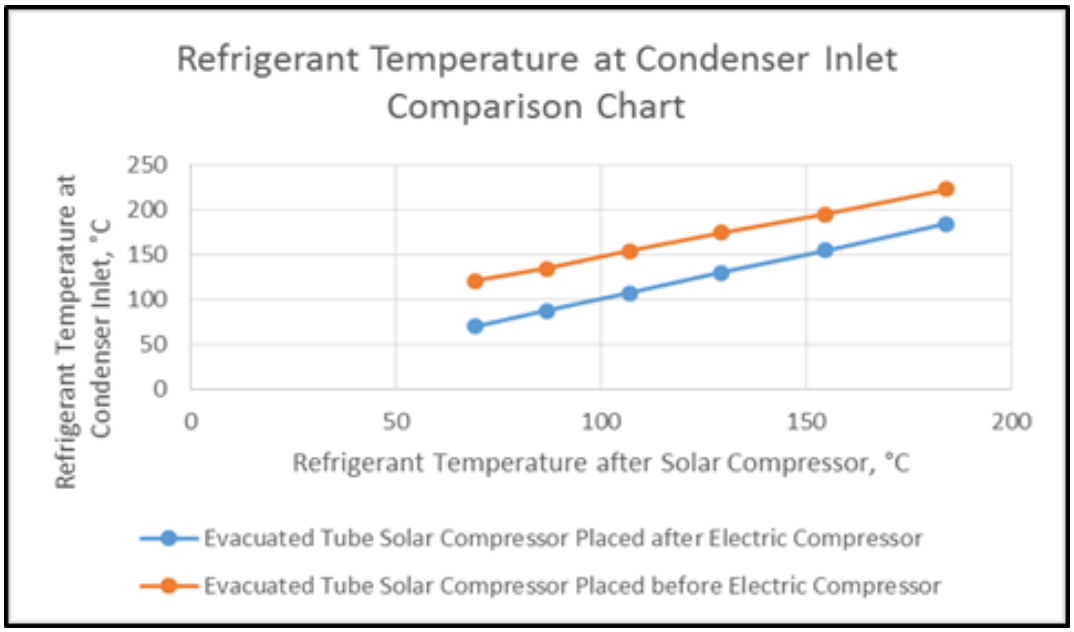

FIGURE 17. Refrigerant temperature comparison for different solar compressor position

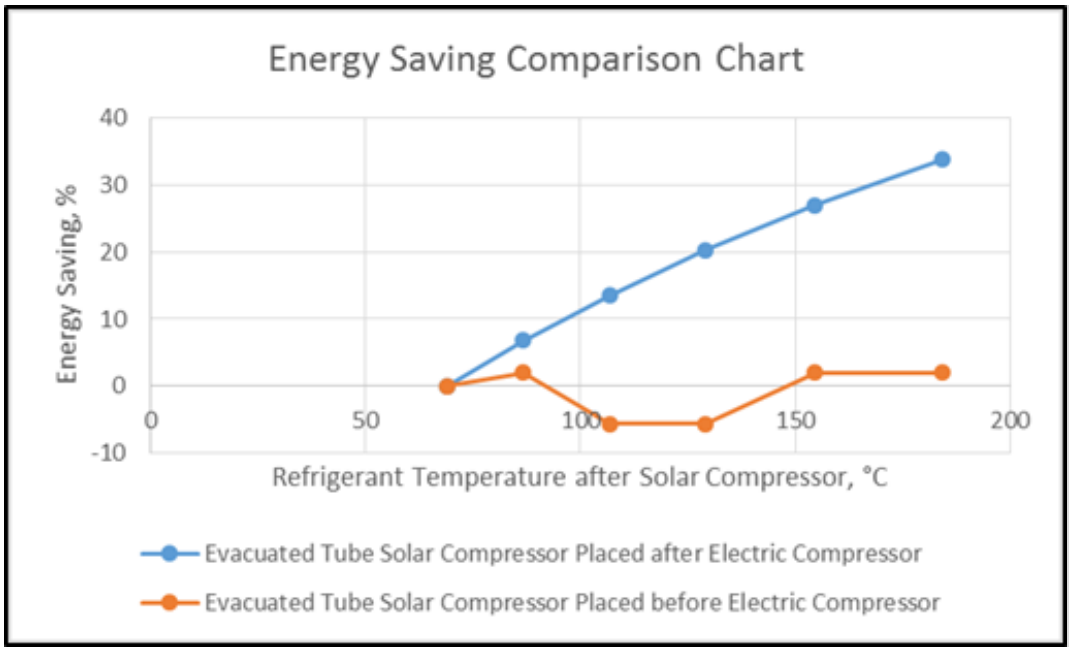

FIGURE 18. Compressor energy saving comparison for different solar compressor position

Both Figure 17 and Figure 18 confirms the advantages of placing solar compressor after electric compressor. For comparison, if solar compressor is placed after electric compressor, the refrigerant temperature entering the condenser is significantly lower, which translates to smaller size condenser. Furthermore, in this configuration, the energy saving increases with the refrigerant temperature. On the other hand, placing the solar compressor before electric compressor provides little to no energy saving due to the high refrigerant temperature requirement.

4.8 ANSYS Simulation

The developed evacuated tube solar collector is a U-tube flow through type.

The simulation is carried out under the following assumptions:

(i) The refrigerant flow is continuous

(ii) The flow is steady and laminar

(iii) The selected longitude, latitude and time zone are 100.9797, 4.3864 and +8 at Universiti Teknologi Petronas as solar calculator input

(iv) Solar ray tracing with fair weather condition model option is selected

(v) Performance is in steady state

(vi) The headers provide uniform flow to tubes

(vii) Dust and dirt on the collector are negligible

Model 1: 12PM (Sample)

The U-tube evacuated tube consists of a copper absorber tube of 1.3m length, with 5mm inner diameter and 2mm thickness. The circular copper tube is covered with 1mm thickness of selective absorber coating to improve tube absorptivity. The U-tube is insulated with circular glass enclosure with 39mm outer diameter and 3mm thickness. The solar collector consists of 12 U-tubes in which the headers provide uniform flow to each tubes. Figure below shows the evacuated tube sizing:

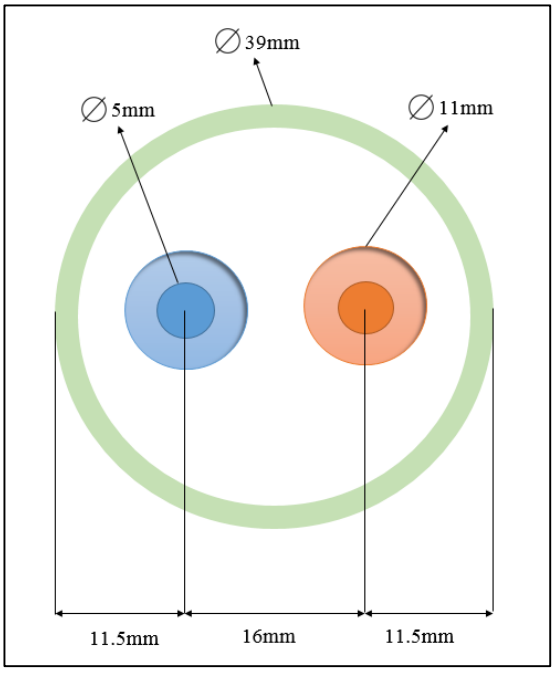

FIGURE 19. U-tube evacuated tube sizing

The refrigerant enters the U-tube evacuated solar collector at 52°C and exits with an average temperature of 166°C.

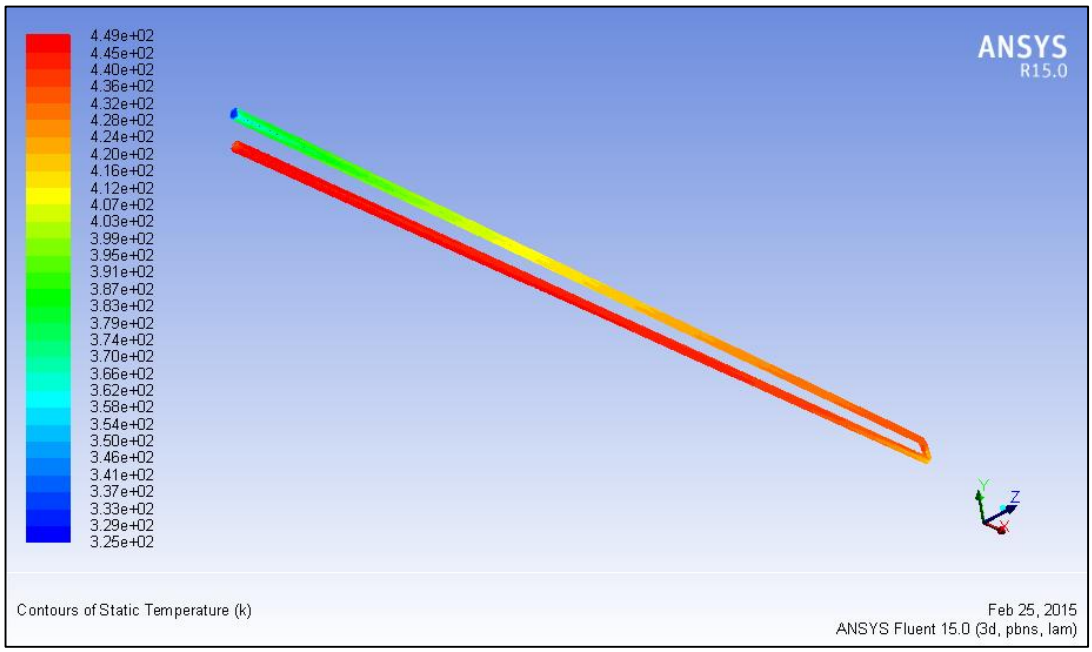

FIGURE 20. Temperature contour of U-tube evacuated solar collector

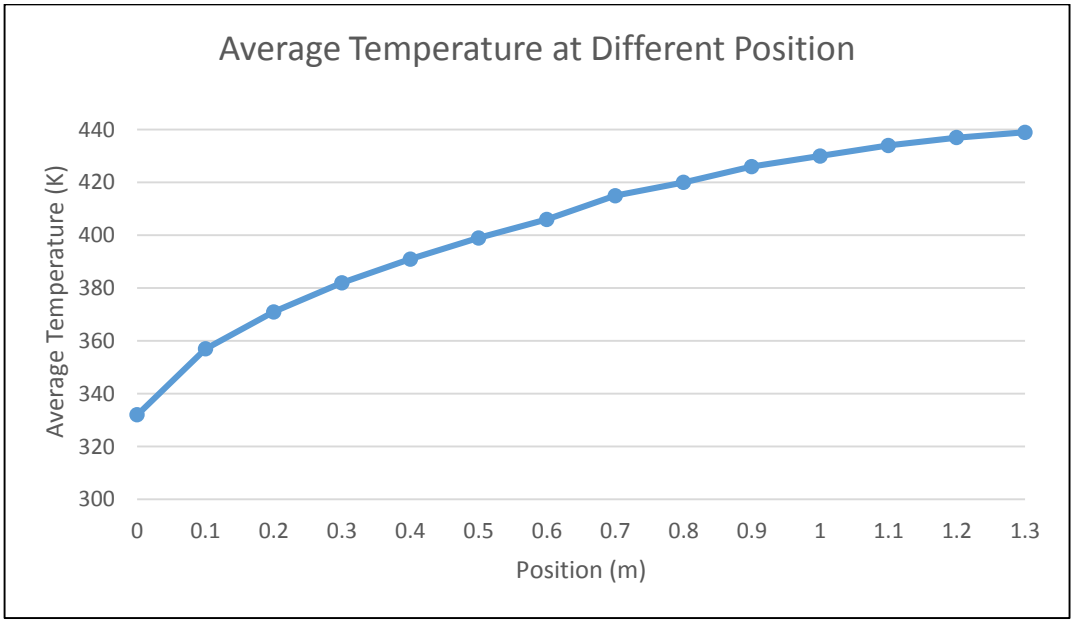

FIGURE 21. Average temperature of refrigerant at different position in U-tube evacuated solar collector

The ANSYS simulation is run extensively to determine the size of evacuated tube solar collector required to achieve at least 160°C of refrigerant temperature in each of the air conditioner model. The tube length and number of tubes indicating the evacuated tube solar collector sizing for each model is shown in the table below:

TABLE 10. Evacuated tube solar collector sizing

	Tube Length (m)	Number of Tubes	Dimension (W x H x D) mm^3
Model 1	0.65	12	580 x 750 x 60
Model 2	0.85	12	580 x 950 x 60
Model 3	0.85	16	780 x 950 x 60
Model 4	0.85	18	875 x 950 x 60
Model 5	0.85	22	1080 x 950 x 60

U-tube evacuated solar collector consists of long copper tube which directs the refrigerant flow through the evacuated tube. This allows a greater heat exchanging area which is highly desirable due to the low thermal conductivity of refrigerant vapour. Figure below shows the schematic diagram of solar collector for model 1:

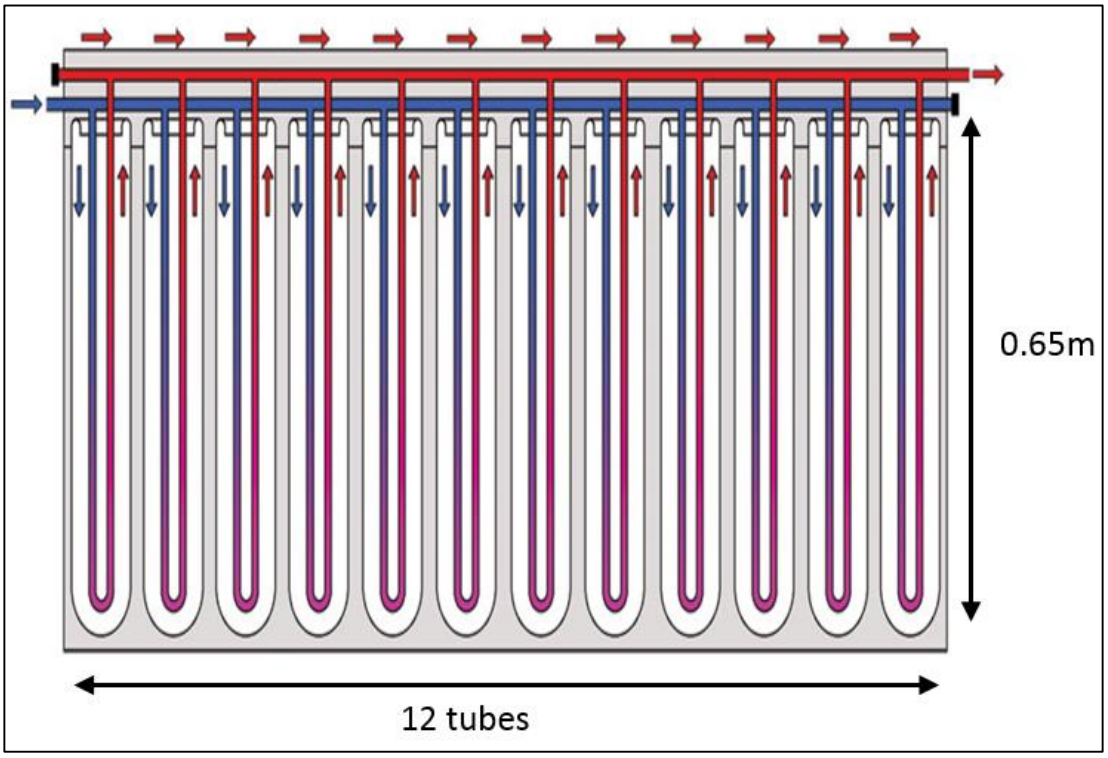

FIGURE 22. Evacuated Tube Solar Collector for Model 1

The solar radiation data at Universiti Teknologi Petronas is generated through Solar Calculator in ANSYS software with longitude, latitude and time zone as 100.9797, 4.3864 and +8 respectively. Solar ray tracing with fair weather condition model option is also selected. The solar radiation at the studied area increases rapidly from 7am and peaks at around 12pm to 2pm and begins to decrease until sunset at around 7pm.

TABLE 11. Solar Radiation at Universiti Teknologi Petronas

Estimated Solar Radiation at UTP			
Time	**W/m2**	**Time**	**W/m2**
1	0	13	874.5
2	0	14	872.8
3	0	15	857.3
4	0	16	822.7
5	0	17	753.8
6	0	18	603.7
7	182.3	19	188.2
8	351.9	20	0
9	659.1	21	0
10	777.9	22	0
11	834.7	23	0
12	863.1	24	0

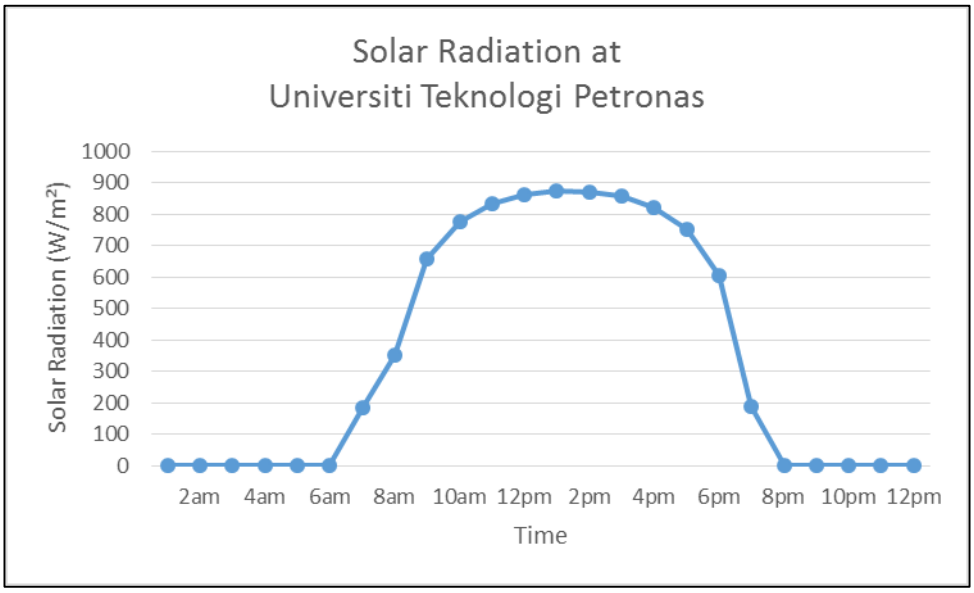

FIGURE 23. Solar Radiation at Universiti Teknologi Petronas

During day time, the energy saving is achieved by both DC compressor and solar compressor. The energy saving increases rapidly from 7am and peaks at around 10am to 4pm and begins to decrease unitl night time. During night time, the absence of solar radiation means energy saving is only contributed by the DC compressor. There is a strong relationship between energy saving and power consumption where the higher the energy saving, the lower the power consumption, and vice versa.

During daytime, Model 5 can achieve the highest maximum energy saving of 44.4%, followed by Model 1, 2, 3 and 4 with energy saving of 37.2%, 35.8%, 34.2% and 36.5% respectively. During nighttime, DC compressor manages energy saving of 25.7% for Model 5, followed by Model 1, 2, 3 and 4 with energy saving of 17.0%, 13.9%, 11.1% and 14.5% respectively. Figure 24 and 25 shows the system energy saving and system power consumption versus time.

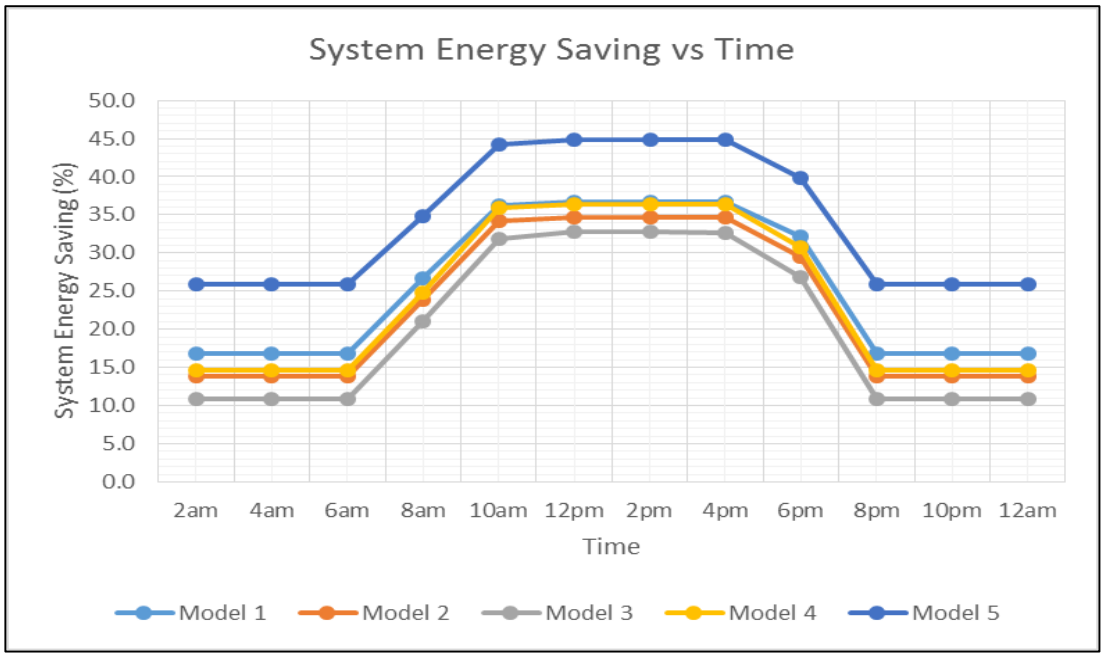

FIGURE 24. Graph of System Energy Saving vs Time

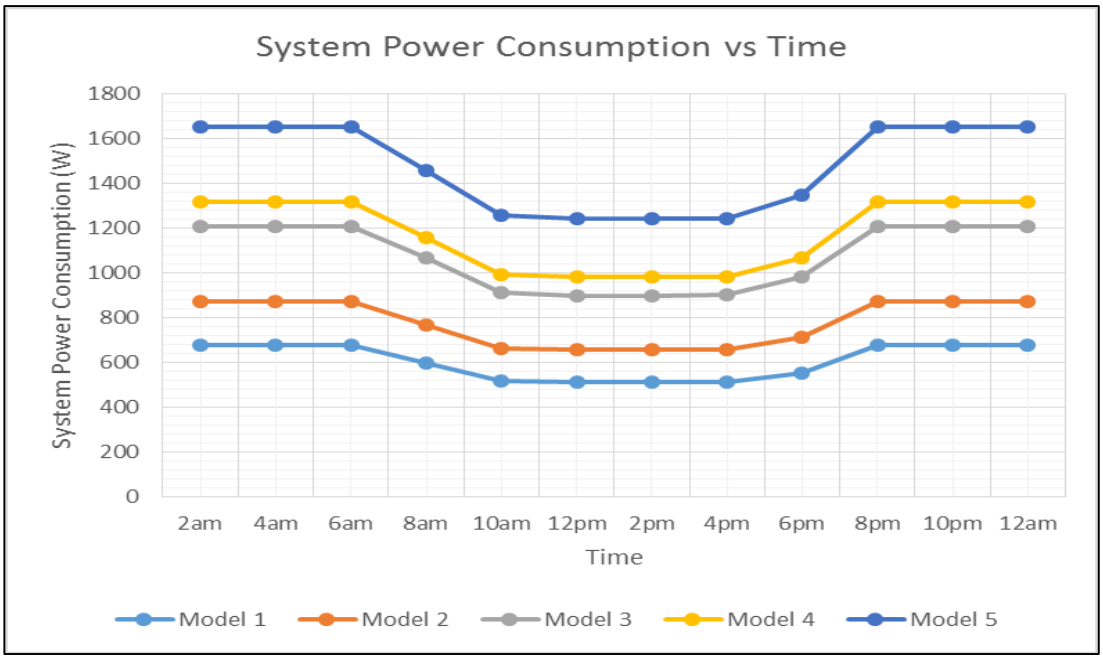

FIGURE 25. Graph of System Power Consumption Saving vs Time

4.9 Discussion on Calculation:

Assumptions:

1. Performance is in steady state
2. The headers provide uniform flow to tubes
3. Dust and dirt on the collector are negligible

The procedure is to estimate the cover temperature, from which $h_{r,t-c}$, $h_{r,c-a}$, and $h_{c,c-a}$ are calculated. These results are then used to calculate T_c from preceding equation. If T_c is close to the initial guess, no further calculations are necessary. Otherwise, the newly calculated T_c is used and the process is repeated.

<u>Model 1: 12 PM (Sample Calculation)</u>

$Solar\ irradiance, G = 865\ W/m^2$

$Copper\ tube\ emittance, \varepsilon_t = 0.07$

$Glass\ cover\ emittance, \varepsilon_c = 0.80$

$Ambient\ temperature, T_a = 30℃$

$Sky\ temperature, T_s = 20℃$

$Mean\ tube\ temperature, T_t = 151\ ℃$

$Estimated\ glass\ cover\ temperature, T_c = 40\ ℃$

(i) Radiation coefficient between the copper tube and the glass cover:

$$h_{r,t-c} = \frac{(5.67x10^{-8})(424^2 + 313^2)(424 + 313)}{\frac{1}{0.07} + \frac{1}{0.80} - 1} = 0.80\, W/m^2 \cdot K$$

(ii) Radiation coefficient for the glass cover to the air:

$$h_{r,c-a} = 0.80(5.67x10^{-8})(313^2 + 293^2)(313 + 293) = 5.05\, W/m^2 \cdot K$$

(iii) Convection coefficient for the glass cover to the air:

$$k = 0.02625\, W/m \cdot K$$

$$\upsilon = 1.655x10^{-5}\, m^2/s$$

$$Pr = 0.7268$$

$$\beta = \frac{1}{T_{avg}} = \frac{1}{308}$$

$$Ra = \frac{9.81\left(\frac{1}{308}\right)(313 - 303)(0.039^3)}{(1.655\, x10^{-5})^2}(0.7268) = 50133.85$$

$$Nu = \left[0.6 + \frac{0.387(50133.85)^{\frac{1}{6}}}{\left[1 + \left(\frac{0.559}{0.7268}\right)^{\frac{9}{16}}\right]^{\frac{8}{27}}}\right]^2 = 6.525$$

$$h_{c,c-a} = \frac{0.02625}{0.039}(0.832) = 4.39\, W/m^2 \cdot K$$

$$U = \left(\frac{1}{(0.0449)(0.80)} + \frac{1}{(0.0398)(5.05 + 4.39)}\right)^{-1} = 0.0327\, W/K$$

$$T_c = 424 - \frac{0.0327\left[\frac{5.05}{5.05 + 4.39}(424 - 293) + \frac{4.39}{5.05 + 4.39}(424 - 303)\right]}{(0.0449)0.80}$$

$$= 308.7\, K = 35.7\, ℃$$

$\therefore$ *New estimated glass cover temperature*, $T_c = 35.7$ ℃

Repeat the calculation with the new estimated glass cover temperature

(i) Radiation coefficient between the copper tube and the glass cover:

$$h_{r,t-c} = \frac{(5.67x10^{-8})(424^2 + 308.7^2)(424 + 308.7)}{\frac{1}{0.07} + \frac{1}{0.80} - 1} = 0.79\, W/m^2 \cdot K$$

(ii) Radiation coefficient for the glass cover to the air:

$$h_{r,c-a} = 0.80(5.67x10^{-8})(308.7^2 + 283^2)(308.7 + 283)$$
$$= 4.94\, W/m^2 \cdot K$$

(iii) Convection coefficient for the glass cover to the air:

$$k = 0.02609\, W/m \cdot K$$
$$\upsilon = 1.635x10^{-5}\, m^2/s$$
$$Pr = 0.7274$$
$$\beta = \frac{1}{T_{avg}} = \frac{1}{305.9}$$
$$Ra = \frac{9.81\left(\frac{1}{305.9}\right)(308.7 - 303)(0.039^3)}{(1.635\, x10^{-5})^2}(0.7274) = 29263.83$$
$$Nu = \left[0.6 + \frac{0.387(29263.83)^{\frac{1}{6}}}{\left[1 + \left(\frac{0.559}{0.7274}\right)^{\frac{9}{16}}\right]^{\frac{8}{27}}}\right]^2 = 5.697$$
$$h_{c,c-a} = \frac{0.02609}{0.039}(5.697) = 3.81\, W/m^2 \cdot K$$

$$U = \left(\frac{1}{(0.0449)(0.79)} + \frac{1}{(0.0398)(4.60 + 2.66)}\right)^{-1} = 0.0321\, W/K$$

$$T_c = 424 - \frac{0.0321\left[\frac{4.94}{4.94 + 3.81}(424 - 293) + \frac{3.81}{4.94 + 3.81}(424 - 303)\right]}{(0.0449)0.79}$$
$$= 309.0\, K = 36.0\, ℃$$

When the cover glass temperature is calculated with this new top loss coefficient, it is found to be 36.0 ℃, which is essentially equal to the estimated of 35.7 ℃.

Heat Loss Calculations:

(i) Copper Tube Heat Loss:

$$\dot{Q}_{t,rad} = h_{r,t-c}\, A_t (T_t - T_c)$$
$$= 0.79(0.0449)(424 - 309.0)$$
$$= 4.06\, W$$

(ii) Glass Cover Heat Loss:

$$\dot{Q}_{c,rad} = h_{r,c-a}\, A_c (T_c - T_s)$$
$$= 4.94(0.0398)(309.0 - 293)$$
$$= 3.08\, W$$

$$\dot{Q}_{c,conv} = h_{c,c-a} A_c (T_c - T_a)$$
$$= 3.81(0.0398)(309.0 - 303)$$
$$= 0.86W$$

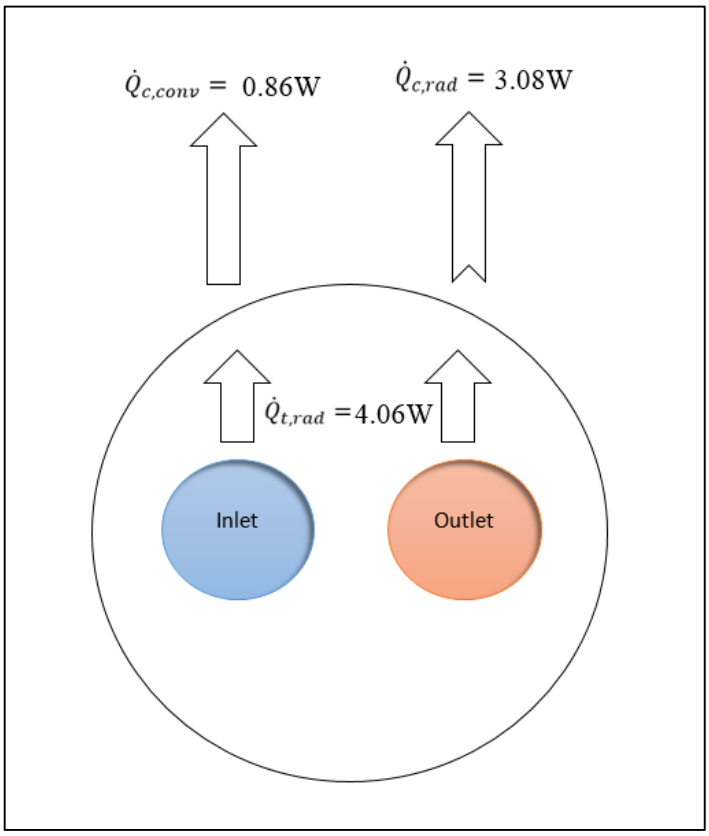

FIGURE 26. Thermal network for U-tube evacuated solar collector

Energy Calculations:

Glass Cover:

- $Transmissivity, \tau = 0.75$
- $Emissivity, \varepsilon_c = 0.80$
- $Reflectivity, \gamma = 0.236$

Copper tube selective absorber coating:

- $Absorptivity, \alpha = 0.94$
- $Emissivity, \varepsilon_t = 0.07$

(i) $\dot{Q}_{total} = \frac{1}{2}\tau\alpha G A_t$

$$= \frac{1}{2}(0.75)(0.94)(865)(0.0449)$$

$$= 13.70\ W$$

(ii) $\dot{Q}_{loss} \approx \dot{Q}_{t,rad} \approx \dot{Q}_{c,rad} + \dot{Q}_{c,conv}$

$\therefore \dot{Q}_{loss} \approx 4.03\ W$

(iii) $\dot{Q}_{gain} = \dot{Q}_{total} - \dot{Q}_{loss}$

$$= 13.70 - 4.03$$

$$= 9.67\ W$$

(iv) $\dot{Q}_{gain} = \dot{m} C_p (T_{out} - T_{in})$

$9.67 = 0.001508333(57.2)(T_{out} - 52)$

$T_{out} = 164.1$ ℃

For Model 1 at 12pm, the calculated refrigerant output temperature is 164.1°C which is essentially equal to the ANSYS simulated output temperature of 166°C. The ANSYS simulation result is further validated with calculations for all five models at different time where the percentage difference is well below 5%. The comparison between calculation and ANSYS simulation is shown in Table 12:

TABLE 12. Refrigerant output temperature after evacuated tube solar collector

		Refrigerant Output Temperature (°C)					
		8am	**10am**	**12pm**	**2pm**	**4pm**	**6pm**
Model 1	**ANSYS**	107.0	157.0	166.0	168.0	161.0	133.0
	Calculation	111.2	157.1	164.1	164.4	159.2	134.2
Model 2	**ANSYS**	107.0	157.0	165.0	167.0	161.0	132.0
	Calculation	103.2	160.0	165.6	165.3	160.4	132.6
Model 3	**ANSYS**	106.0	155.0	163.0	167.0	159.0	131.0
	Calculation	103.2	155.9	164.4	165.3	156.2	132.6
Model 4	**ANSYS**	107.0	157.0	165.0	167.0	160.0	132.0
	Calculation	103.7	155.6	165.6	165.2	160.4	132.6
Model 5	**ANSYS**	107.0	156.0	164.0	167.0	160.0	132.0
	Calculation	105.1	155.8	164.5	165.8	160.2	131.9

4.10 Performance comparison with manufacturer's data sheet

The performance of the research solar hybrid air conditioning system is compared with the SolAir World Hybrid Solar Air Conditioning System. SolAir World International is an established international company delivering solar air conditioning that provides an innovative energy saving air conditioner by utilising thermal energy to provide cost effective clean green thermal air conditioning comfort. Table 13 and 14 shows the performance of both research and SolAir World solar hybrid air conditioner where the latter is tested under Australia weather condition.

TABLE 13. Solar Hybrid Air Conditioner Performance

Model	**1**	**2**	**3**	**4**	**5**
Capacity (btu/h)	10000	13000	18000	19500	24000
Power Input (W)	510-677	655-873	899-1209	983-1316	1243-1655

TABLE 14. SolAir World Hybrid Solar AC Specification – Wall Mounted Units (SolAir World International, 2014)

Model	**SWWR-26GV**	**SWWR-35GV**	**SWWR-56GV**	**SWWR-60GV**	**SWWR-72GV**
Capacity (btu/h)	9000	12000	19000	20000	24000
Power Input (W)	500-680	560-800	1040-1260	1280-1400	1490-1680

From the above data, Model SWWR-26GV from SolAir World has capacity of 9000btu/h and requires power input of 500-680W, while Model 1 has slightly higher capacity of 10000btu/h but only requires about the same power input of 510-677W.

Next, Model SWWR-35GV from SolAir World has capacity of 12000btu/h and requires power input of 560-800W, while Model 2 has slightly higher capacity of 13000btu/h and requires slightly higher power input of 655-873W.

Following, Model SWWR56GV from SolAir World has capacity of 19000btu/h and requires power input of 1040-1260W, while Model 3 has a lower capacity of 18000btu/h and requires slightly lower power input of 899-1209W.

Next, Model SWWR-60GV from SolAir World has capacity of 20000btu/h while drawing power input of 1280-1400W. Meanwhile, Model 4 sits between Model SWWR-56GV and Model SWWR-60GV and has capacity of 19500btu/h and requires power input of 983-1316W.

Lastly, both Model SWWR-72GV from SolAir World and Model 5 has capacity of 24000btu/h, with power requirement of 1490-1680W and 1243-1655W respectively.

Overall, the research solar hybrid air conditioning system shows a comparable performance with the SolAir World system. This indicates the high practicality of solar hybrid air conditioning system in Malaysia.

4.11 Cost Analysis

The solar hybrid air conditioning system is evaluated on the electricity bill saving based on 3 operating cycle, typically the office hours, sleeping hours and 24 hours. Offiice hour cycle is from 8am to 6pm while sleeping hour cycle is from 10pm to 6am. The cost analysis is based on TNB electric tariff of RM0.33/kWh. (Tenaga National Berhad Tariff Plan, 2014)

Model 1: Sample Calculation

(i) Air conditioner running from 8AM to 6PM (Office)

TABLE 15. Solar Hybrid Air Conditioning System Performance (8am-6pm)

Time	**Energy Saving (%)**	**Power Input (W)**
8am	26.7	595.1
10am	36.2	514.4
12pm	36.7	510.6
2pm	36.7	510.6
4pm	36.7	510.6
6pm	32.1	549.2
Avg	**34.2**	**531.8**

TABLE 16. Air Conditioner Saving Comparison (8am-6pm)

	Power (W)	**Power Consumption/month (kWh)**	**Electricity Bill (RM)**
Conventional air conditioning system	815.0	244.5	80.69
Solar hybrid air conditioning system	531.8	159.5	52.65
Saving	**283.2**	**85.0 (34.8%)**	**28.04**

From the calculations for Model 1, operating from 8am to 6pm which is typically office hours, the solar hybrid air conditioning system is able to achieve 34.8% of energy saving which is equivalent to power consumption of 283.2W less than the conventional unit. Throughout the month, the solar hybrid air conditioner consumes 85.0kWh less than the conventional unit, contributing to electricity bill saving of RM28.04 per month.

(ii) Air conditioner running from 10PM to 6AM (Bedroom)

TABLE 17. Solar Hybrid Air Conditioning System Performance (10pm-6am)

Time	**Energy Saving (%)**	**Power Input (W)**
10pm	16.8	677.0
12am	16.8	677.0
2am	16.8	677.0
4am	16.8	677.0
6am	16.8	677.0
Avg	**16.8**	**677.0**

TABLE 18. Air Conditioner Saving Comparison (10pm-6pm)

	Power (W)	**Power Consumption/month (kWh)**	**Electricity Bill (RM)**
Conventional air conditioning system	815.0	195.6	64.55
Solar hybrid air conditioning system	677.0	162.5	53.63
Saving	**138.0**	**33.1 (16.8%)**	**10.92**

From the calculations for Model 1, operating from 10pm to 6am which is typically sleeping hours, the solar hybrid air conditioning system is able to achieve 16.8% of energy saving which is equivalent to power consumption of 138.0W less than the conventional unit. The lower energy saving performance is due to the absence of sunlight at night time. Throughout the month, the solar hybrid air conditioner consumes 33.1kWh less than the conventional unit, contributing to electricity bill saving of RM10.92 per month.

(iii) Air conditioner running 24 hours

TABLE 19. Solar Hybrid Air Conditioning System Performance (24hours)

Time	**Energy Saving (%)**	**Power Input (W)**
12am	16.8	677.0
2am	16.8	677.0
4am	16.8	677.0
6am	16.8	677.0
8am	26.7	595.1
10am	36.2	514.4
12pm	36.7	510.6
2pm	36.7	510.6
4pm	36.7	510.6
6pm	32.1	549.2
8pm	16.8	677.0
10pm	16.8	677.0
Avg	**25.5**	**604.4**

TABLE 20. Air Conditioner Saving Comparison (24hours)

	Power (W)	**Power Consumption/month (kWh)**	**Electricity Bill (RM)**
Conventional air conditioning system	815.0	586.8	193.64
Solar hybrid air conditioning system	604.4	435.2	143.62
Saving	**210.6**	**151.6 (25.8%)**	**50.02**

From the calculations for Model 1, operating for 24 hours, the solar hybrid air conditioning system is able to achieve 25.8% of energy saving which is equivalent to power consumption of 210.6W less than the conventional unit. Throughout the month, the solar hybrid air conditioner consumes 151.6kWh less than the conventional unit, contributing to electricity bill saving of RM50.02 per month.

The table below shows the summary of power consumption and total saving for each air conditioner model, operating at 3 different cycles typically the office hours, sleeping hours and 24 hours. The total saving increases with the capacity of the air conditioner. Therefore, Model 5 has the highest total saving, while Model 1 has the least total saving.

TABLE 21. Solar Hybrid Air Conditioner Saving Summary

		Power Consumption/month (kWh)		**Saving**	
		Normal air conditioning system	Solar hybrid air conditioning system	Total energy saving per month (kWh)	Total saving per month (RM)
Model 1	8am-6pm	244.5	159.5	85.0 (34.8%)	28.04
	10pm-6am	195.6	162.5	33.1 (16.8 %)	10.92
	24 hours	586.8	435.2	151.6 (25.8%)	50.02
Model 2	8am-6pm	304.5	207.1	97.4 (32.0%)	32.14
	10pm-6am	243.6	210.0	33.6 (13.8%)	11.09
	24 hours	730.8	563.4	167.4 (22.9%)	55.24
Model 3	8am-6pm	408.0	286.8	121.2 (29.7%)	40.00
	10pm-6am	326.4	290.8	35.6 (10.9%)	11.75
	24 hours	979.2	780.4	198.8 (20.3%)	65.60
Model 4	8am-6pm	462.0	307.7	154.3 (33.4%)	50.92
	10pm-6am	369.6	315.6	54.0 (14.6%)	17.82
	24 hours	1108.8	842.7	266.1 (24.0%)	87.81
Model 5	8am-6pm	669.0	386.0	283.0 (42.3%)	93.39
	10pm-6am	535.2	396.6	138.6 (25.9%)	45.74
	24 hours	1605.6	1058.1	547.5 (34.1%)	180.68

TABLE 22. Conventional and solar hybrid air conditioner estimated price (Yuen Kong Electrical & Ningbo Soenbo Energy Technology, 2015)

	Conventional Air Conditioner	**Solar Hybrid Air Conditioner**
	Estimated Price (RM)	**Estimated Price (RM)**
Model 1	930	2700
Model 2	1190	3480
Model 3	1970	4950
Model 4	2100	5200
Model 5	2280	6150

From data in Table 21 and 22, breakeven analysis done to determine the financial feasibility of the solar hybrid air conditioning system. Breakeven point is defined as the required time for the solar hybrid air conditioner to shows its cost advantages over the conventional unit. The air conditioners are assumed to be operating at both office hour (8am-6pm) and sleeping hour (10pm-6am). The breakeven analysis for each model are shown in Figure 27, 28, 29, 30 and 31.

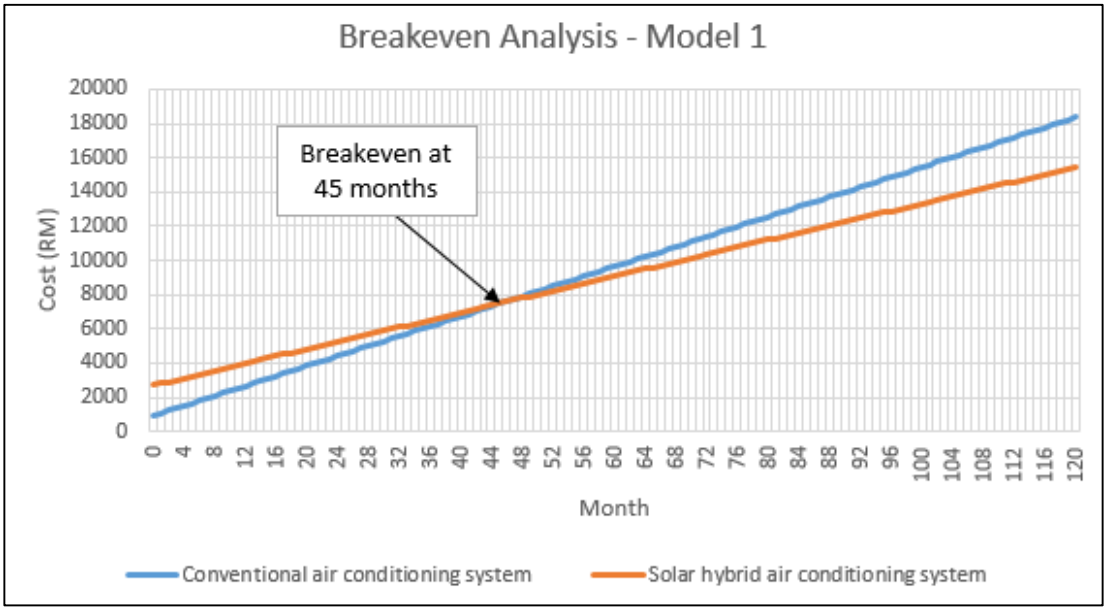

FIGURE 27. Breakeven analysis - Model 1

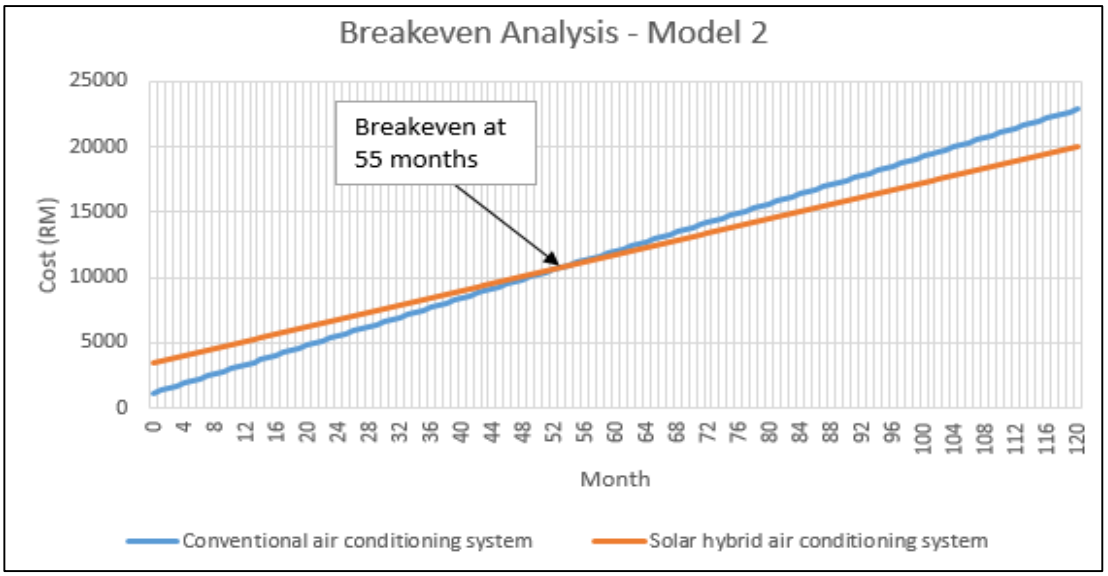

FIGURE 28. Breakeven analysis - Model 2

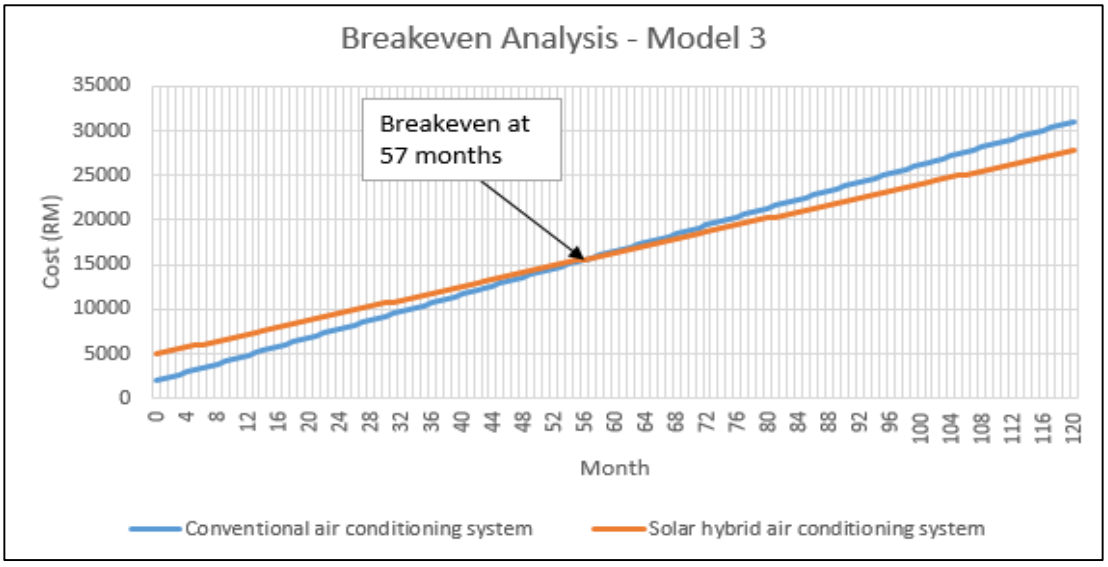

FIGURE 29. Breakeven analysis - Model 3

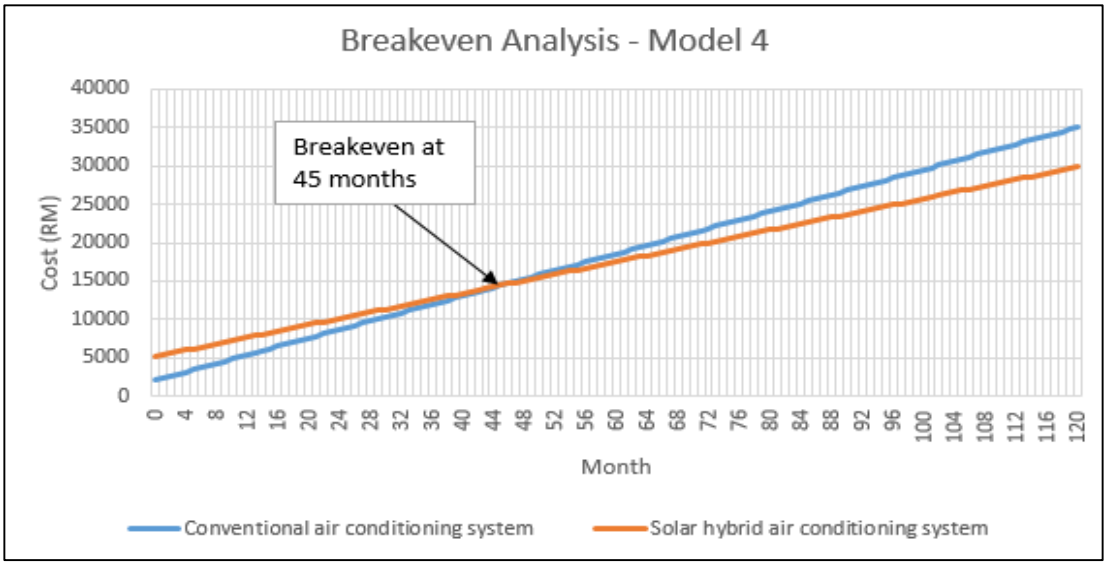

FIGURE 30. Breakeven analysis - Model 4

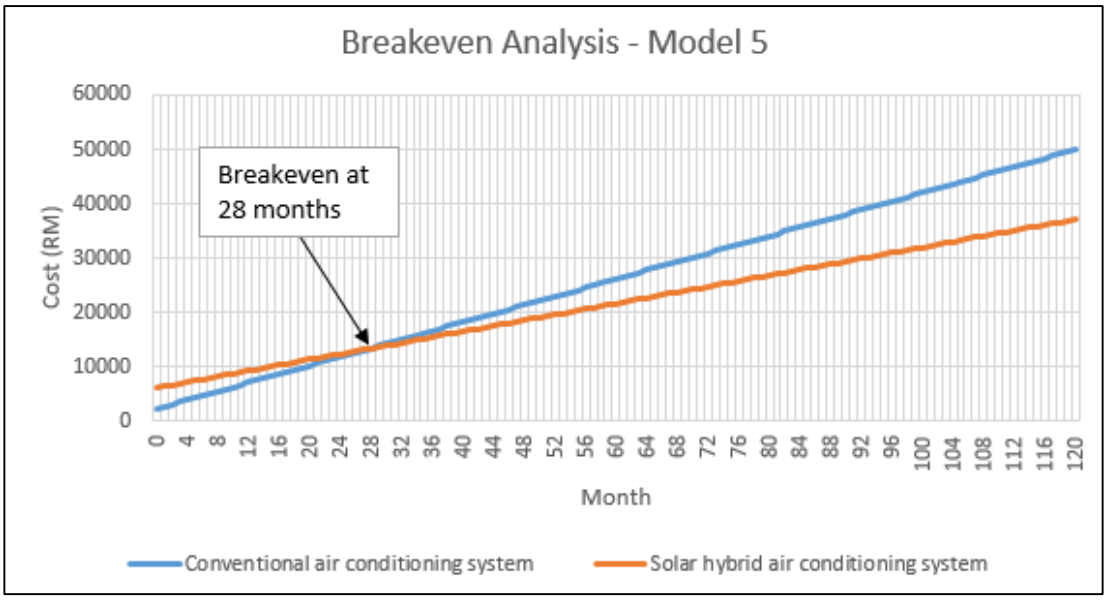

FIGURE 31. Breakeven analysis - Model 5

From the breakeven analysis graphs, Model 5 has the shortest breakeven point at 28 months, followed by Model 1 and 4 at 45 months. Next, Model 2 has breakeven point at 55 months. Lastly, Model 3 has the longest breakeven point at 57 months. The solar hybrid air conditioner is initially priced at higher price tag. However, lower electricity consumption makes it more economical in the long run. Generally, the solar hybrid air conditioner can achieve breakeven within 2 to 5 years, depending on usage.

CHAPTER 5

CONCLUSION AND RECOMMENDATION

Solar air conditioning system is a great innovation which pushes solar energy leaps ahead while promoting positive impact on the environment. Solar Hybrid Air Conditioning System is able to achieve up to 45% energy saving during daytime, thus significantly reduces the electricity peak load during the day. Meanwhile, the DC compressor will contribute up to 25% of energy saving during night time. In addition, Microsoft Excel spreadsheet is also prepared to facilitate the calculation of refrigerant temperature and energy saving of the system. Furthermore, the project also proved the practicality of solar hybrid air conditioning system in Malaysia. The main modifications needed are DC compressor, higher capacity condenser and evacuated tube solar collector. Despite the higher price tag, the solar hybrid air conditioner can achieve breakeven within 2 to 5 years. Thermal storage and photovoltaic system to provide full off grid performance are suggested for future development.

REFERENCES

Admiraal D.M. and Bullard C.W. 1993, *Heat Transfer in Refrigerator Condensers and Evaporators*, Thesis, University of Illinois, Urbana

Ali B.H., Gilani S.I. and Hussain H.K. 2014, *A Three Dimensional Performance Analysis of a Developed Evacuated Tube Collector using a CFD Fluent Solar Load Model*, Thesis, Universiti Teknologi Petronas, Malaysia.

Ali A., Hwang Y.H. and Radermacher R. 2013, *Review of Solar Thermal Air Conditioning Technologies*, Thesis, The Petroleum Institute and University of Maryland, United Arab Emirates and USA.

Anand S., Gupta A. and Tyagi S.K. 2013, *Renewable energy powered evacuated tube collector refrigerator system*, Thesis, Shri Mata Vaishno Devi University, India

Borhanazad H., Mekhilef S., Saidur R. and Boroumandjazi G. 2013, *Potential application of renewable energy for rural electrification in Malaysia*, Thesis, University of Malaya, Malaysia

Brown J.S., Domanski P.A. and Lemmon E.W. 2007, *Theoretical Vapor Compression Cycle Design Program*, Thesis, National Institute of Standards and Technology, Gaithersburg.

Budihardjo I. and Morrison G.L. 2008, *Performance of water-in-glass evacuated tube solar water heaters*, Thesis, University of New South Wales, Australia

Cengel Y.A. and Ghajar A.J. 2013, *Heat and Mass Transfer, Fundamentals and Applications*, Singapore, Mc Graw Hill

Cengel Y, Boles M. 2002, *Thermodynamics: An Engineering Approach.* Dubuque, Iowa: McGraw-Hill.

Concentrated Solar Thermal: Collecting Heat from the Sun. 2013 [cited 2014 11 October]; Available from http://www.greenrhinoenergy.com/solar/technologies/cst_technologies.php

Daut I., Adzrie M., Irwanto M., Ibrahim P. and Fitra M. 2013, *Solar Powered Air Conditioning System*, Thesis, Universiti Malaysia Perlis, Malaysia

Demma D. 2005, *The Pressure-Enthalpy Chart*, Report, Parker Hannifin Corporation, Washington

Duffie J.A. and Beckman W.A. 2006, *Solar Engineering of Thermal Process*, New Jersey, John Wiley & Sons

Eicker U. 2003, *Solar Technologies for Buildings*, Chichester, John Wiley & Sons Ltd

Enteria N. and Akbarzadeh A. 2014, *Solar Energy Sciences and Engineering Applications*, London, CRC Press Taylor & Francis Group

Foster R., Ghassemi M. and Cota A. 2010, *Solar Energy, Renewable Energy and the Environment*, New York, CRC Press

Granet I. and Bluestein M. 2004, *Thermodynamics and Heat Power,* Columbus, Pearson Education Ltd

Henning H.M. 2007, *Solar Assisted Air Conditioning in Buildings*, Austria, Springer-Verlag Wien New York.

Hooshang M., Moghadam R.A., Nia S.A., Masouleh M.T. 2014, *Optimization of Stirling engine design parameters using neural networks.* Thesis, University of Tehran, Iran

Hossain, M.S., Saidur R., Fayaz H. and Ahamed J.U. 2011, *Review on solar water heater collector and thermal energy performance of circulating pipe,* Thesis, University of Malaya, Malaysia

Hybrid Solar Air Conditioning. 2011 [cited 2014 10 October]; Available from http://www.machine-history.com/Solar%20Powered%20Air%20Conditioning

Jafarkazemi F. and Abdi H. 2012, *Evacuated tube solar heat pipe collector model and associated tests*, Thesis, Islamic Azad University, Iran

Kalkan N., Young E.A. and Celiktas A. 2011, *Solar Thermal Air Conditioning Technology Reducing the Footprint of Solar Thermal Air Conditioning*, Thesis, University of Southampton, United Kingdom.

Kalogirou S.A. 2014, *Solar Energy Engineering, Processes and Systems*, Oxford, Academic Press Elsevier Inc

Karim A.M., Kasaeian A. and Kaabinejadian A. 2014, *Performance Investigation of Solar Evacuated Tube Collector Using TRNSYS in Tehran*, Thesis, University of Tehran, Iran

Klein S.A. 1992, *Design Considerations for Refrigeration Cycles,* Thesis, University of Wisconsin, Madison

Kohlenbach P. and Jakob U. 2014, *Solar Cooling, The Earthscan Expert Guide to Solar Cooling Systems,* Glasgow, Bell & Bain Ltd

Lamanna B. 2010, *Inverter and programmable controls in heat pump applications*, Report, Carel Industries, Brussels

Malaysia Primary Energy Supply Summary [cited 2014 10 December]; Available from http://meih.st.gov.my/statistics

Moorthy M. 2010, *Performance of Solar Air Conditioning System using Heat Pipe Evacuated Tube Collector,* Thesis, Universiti Malaysia Pahang, Malaysia

National Renewable Energy Policy & Action Plan. 2008. Kementerian Tenaga, Teknologi Hijau dan Air, Malaysia

Norwood Z.M. 2011, *Designing a Distributed Concentrating Solar Combined Heat and Power System,* Thesis, University of California, Berkeley

Ochi, M.; and Ohsumi, K. 1989, *Fundamental of Refrigeration and Air Conditioning.* Ochi Engineering Consultant Office.

Ong K.S. and Tong W.L. 2012, *System Performance of U-tube and Heat Pipe Solar Water Heater,* Thesis, Monash University Sunway Campus, Malaysia

Robert P. 2008, *High Temperature Solar Concentrators.* Thesis, Institute of Technical Thermodynamics, Germany

Rona N. 2004, *Solar air conditioning systems; focus on components and their working principles*. M.Sc. Thesis. Chalmers University of Technology.

Ross A. 2011, *Making Stirling Engines*, Ross Experimental

Solar Evacuated Tube Collectors, Report, Navitron Ltd, United Kingdom

Thermodynamic Properties of DuPont Freon 22 (R-22) Refrigerant, DuPont Fluorochemicals, Wilmington

Thorpe D. 2011, *Solar Technology, The Earthscan Expert Guide to using Solar Energy for Heating, Cooling and Electricity*, London, Bell & Bain Ltd

Tiwari G.N. 2013, *Solar Energy Fundamentals, Design, Modelling and Applications,* Oxford, Alpha Science International Ltd

Wang S.K. and Lavan Z. 1999, *Mechanical Engineering Handbook, Air Conditioning and Refrigeration,* CRC Press LLC

APPENDICES

Appendix 1: R22 Superheated Vapour – Constant Pressure Table

Temp °C	500 (+0.12°C)			525 (+1.63°C)			550 (+3.09°C)			575 (+4.50°C)			Temp °C
	V	H	S	V	H	S	V	H	S	V	H	S	
	(0.0469)	(405.1)	(1.750)	(0.0448)	(405.6)	(1.748)	(0.0428)	(406.2)	(1.746)	(0.0410)	(406.7)	(1.744)	
5	0.0482	408.7	1.764	0.0456	408.1	1.757	0.0432	407.6	1.751	0.0411	407.1	1.746	5
10	0.0494	412.3	1.777	0.0468	411.8	1.771	0.0444	411.3	1.765	0.0422	410.8	1.759	10
15	0.0506	416.0	1.789	0.0479	415.5	1.783	0.0455	415.0	1.778	0.0433	414.6	1.772	15
20	0.0518	419.6	1.802	0.0491	419.2	1.796	0.0466	418.7	1.790	0.0444	418.3	1.785	20
25	0.0530	423.2	1.814	0.0502	422.8	1.808	0.0477	422.4	1.803	0.0454	422.0	1.797	25
30	0.0541	426.8	1.826	0.0513	426.4	1.820	0.0488	426.0	1.815	0.0465	425.6	1.810	30
35	0.0553	430.4	1.838	0.0524	430.1	1.832	0.0498	429.7	1.827	0.0475	429.3	1.822	35
40	0.0564	434.1	1.849	0.0535	433.7	1.844	0.0509	433.4	1.839	0.0485	433.0	1.834	40
45	0.0575	437.7	1.861	0.0546	437.4	1.855	0.0519	437.0	1.850	0.0495	436.7	1.845	45
50	0.0586	441.3	1.872	0.0557	441.0	1.867	0.0530	440.7	1.862	0.0505	440.4	1.857	50
55	0.0597	445.0	1.884	0.0567	444.7	1.878	0.0540	444.4	1.873	0.0515	444.0	1.868	55
60	0.0608	448.6	1.895	0.0578	448.3	1.889	0.0550	448.0	1.884	0.0524	447.7	1.879	60
65	0.0619	452.3	1.906	0.0588	452.0	1.900	0.0560	451.7	1.895	0.0534	451.5	1.890	65
70	0.0630	456.0	1.916	0.0598	455.7	1.911	0.0570	455.5	1.906	0.0543	455.2	1.901	70
75	0.0640	459.7	1.927	0.0609	459.4	1.922	0.0579	459.2	1.917	0.0553	458.9	1.912	75
80	0.0651	463.4	1.938	0.0619	463.2	1.932	0.0589	462.9	1.927	0.0562	462.7	1.923	80
85	0.0662	467.2	1.948	0.0629	466.9	1.943	0.0599	466.7	1.938	0.0572	466.4	1.933	85
90	0.0672	470.9	1.959	0.0639	470.7	1.953	0.0609	470.5	1.949	0.0581	470.2	1.944	90
95	0.0683	474.7	1.969	0.0649	474.5	1.964	0.0618	474.2	1.959	0.0590	474.0	1.954	95
100	0.0693	478.5	1.979	0.0659	478.3	1.974	0.0628	478.0	1.969	0.0600	477.8	1.964	100
105	0.0704	482.3	1.989	0.0669	482.1	1.984	0.0638	481.9	1.979	0.0609	481.7	1.975	105
110	0.0714	486.1	1.999	0.0679	485.9	1.994	0.0647	485.7	1.989	0.0618	485.5	1.985	110
115	0.0724	490.0	2.009	0.0689	489.8	2.004	0.0657	489.6	1.999	0.0627	489.4	1.995	115
120	0.0735	493.8	2.019	0.0699	493.7	2.014	0.0666	493.5	2.009	0.0636	493.3	2.005	120
125	0.0745	497.7	2.029	0.0709	497.6	2.024	0.0675	497.4	2.019	0.0645	497.2	2.015	125
130	0.0755	501.7	2.039	0.0718	501.5	2.034	0.0685	501.3	2.029	0.0654	501.1	2.024	130
135	0.0766	505.6	2.049	0.0728	505.4	2.044	0.0694	505.2	2.039	0.0663	505.1	2.034	135
140	0.0776	509.5	2.058	0.0738	509.4	2.053	0.0704	509.2	2.048	0.0672	509.0	2.044	140
145	0.0786	513.5	2.068	0.0748	513.3	2.063	0.0713	513.2	2.058	0.0681	513.0	2.053	145
150	0.0796	517.5	2.077	0.0757	517.3	2.072	0.0722	517.2	2.068	0.0690	517.0	2.063	150
155	0.0806	521.5	2.087	0.0767	521.4	2.082	0.0731	521.2	2.077	0.0699	521.0	2.072	155

TABLE 23. R22 Superheated Vapour - Constant Pressure Table

Temp °C	1400 (36.31°C)			1500 (39.10°C)			1600 (41.75°C)			1700 (44.28°C)			Temp °C
	V	H	S	V	H	S	V	H	S	V	H	S	
	(0.0167)	(415.6)	(1.703)	(0.0155)	(416.1)	(1.700)	(0.0144)	(416.5)	(1.696)	(0.0135)	(416.9)	(1.693)	
40	0.0171	419.1	1.714	0.0156	417.0	1.702	-	-	-	-	-	-	40
45	0.0177	423.7	1.729	0.0162	421.8	1.718	0.0148	419.8	1.706	0.0136	417.6	1.695	45
50	0.0183	428.2	1.743	0.0167	426.4	1.732	0.0153	424.6	1.721	0.0141	422.6	1.711	50
55	0.0188	432.5	1.756	0.0172	430.9	1.746	0.0159	429.2	1.736	0.0146	427.5	1.726	55
60	0.0193	436.9	1.769	0.0177	435.4	1.759	0.0164	433.8	1.750	0.0151	432.2	1.740	60
65	0.0198	441.1	1.782	0.0182	439.7	1.772	0.0168	438.3	1.763	0.0156	436.8	1.754	65
70	0.0203	445.3	1.795	0.0187	444.0	1.785	0.0173	442.7	1.776	0.0160	441.2	1.767	70
75	0.0208	449.5	1.807	0.0192	448.3	1.797	0.0177	447.0	1.788	0.0165	445.7	1.780	75
80	0.0213	453.7	1.819	0.0196	452.5	1.809	0.0182	451.3	1.801	0.0169	450.0	1.792	80
85	0.0217	457.8	1.830	0.0201	456.7	1.821	0.0186	455.6	1.813	0.0173	454.4	1.804	85
90	0.0222	462.0	1.842	0.0205	460.9	1.833	0.0190	459.8	1.824	0.0177	458.7	1.816	90
95	0.0226	466.1	1.853	0.0209	465.1	1.844	0.0194	464.0	1.836	0.0181	463.0	1.828	95
100	0.0231	470.2	1.864	0.0213	469.2	1.855	0.0198	468.2	1.847	0.0185	467.2	1.839	100
105	0.0235	474.3	1.875	0.0218	473.4	1.866	0.0202	472.4	1.858	0.0189	471.5	1.851	105
110	0.0239	478.4	1.886	0.0222	477.5	1.877	0.0206	476.6	1.869	0.0193	475.7	1.862	110
115	0.0244	482.6	1.896	0.0226	481.7	1.888	0.0210	480.8	1.880	0.0196	479.9	1.873	115
120	0.0248	486.7	1.907	0.0230	485.8	1.899	0.0214	485.0	1.891	0.0200	484.1	1.884	120
125	0.0252	490.8	1.917	0.0234	490.0	1.909	0.0218	489.2	1.902	0.0204	488.3	1.894	125
130	0.0256	494.9	1.928	0.0238	494.1	1.920	0.0222	493.4	1.912	0.0207	492.6	1.905	130
135	0.0260	499.1	1.938	0.0242	498.3	1.930	0.0225	497.5	1.922	0.0211	496.8	1.915	135
140	0.0265	503.2	1.948	0.0246	502.5	1.940	0.0229	501.7	1.933	0.0214	501.0	1.925	140
145	0.0269	507.4	1.958	0.0249	506.7	1.950	0.0233	505.9	1.943	0.0218	505.2	1.936	145
150	0.0273	511.5	1.968	0.0253	510.9	1.960	0.0236	510.2	1.953	0.0221	509.5	1.946	150
155	0.0277	515.7	1.978	0.0257	515.1	1.970	0.0240	514.4	1.963	0.0225	513.7	1.956	155
160	0.0281	519.9	1.987	0.0261	519.3	1.980	0.0243	518.6	1.972	0.0228	518.0	1.965	160
165	0.0285	524.1	1.997	0.0264	523.5	1.989	0.0247	522.9	1.982	0.0231	522.2	1.975	165
170	0.0289	528.3	2.007	0.0268	527.7	1.999	0.0250	527.1	1.992	0.0235	526.5	1.985	170
175	0.0292	532.6	2.016	0.0272	532.0	2.009	0.0254	531.4	2.001	0.0238	530.8	1.995	175
180	0.0296	536.8	2.026	0.0276	536.2	2.018	0.0257	535.6	2.011	0.0241	535.1	2.004	180
185	0.0300	541.1	2.035	0.0279	540.5	2.027	0.0261	539.9	2.020	0.0245	539.4	2.014	185
190	0.0304	545.3	2.044	0.0283	544.8	2.037	0.0264	544.2	2.030	0.0248	543.7	2.023	190

TABLE 24. R22 Superheated Vapour - Constant Pressure Table (cont')

Appendix 2: U-tube Evacuated tube solar collector product data sheet

SunMaxx Solar™
Hot Water Solutions

PRODUCT DATA SHEET
ThermoPower VDF Vacuum Tube Collector

1) Manifold
2) Double Wall Vacuum Tube
3) 1/4" Male NPT Brass Connection
4) Temperature Sensor Well
5) Free Standing Extruded Aluminum Adjustable Frame

Technical Specifications

Tube Length	59 in.
Outer Tube Diameter	1.46 in.
Tube Thickness	0.1 in.
Tube Material	Borosilicate Glass
Tube Coating	Al - N/Al
Thermal Expansion	3.3 x 10^{-6}
Absorption Efficiency	> 94%
Emittance	< 7%
Vacuum	P < 5x10^{-3} Pa
Heat Loss	< 0.7 W/m²C
Maximum Strength	1.0
Stagnation Temperature	428 °F
Flow Rate	0.4 - 0.6 gpm [1]
Fittings	1/2 in. NPT

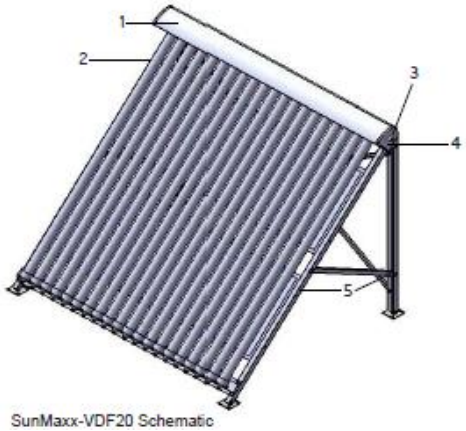

SunMaxx-VDF20 Schematic

FIGURE 32. U-tube Evacuated tube solar collector product data sheet

Appendix 3: Microsoft Excel Calculation Spreadsheet (Model 1 – 12PM)

1st Iteration					
Data		(°C)		Constant	
ε_t	0.07			g	9.81
ε_c	0.8			σ	5.67E-08
T_a	30	303			
T_s	20	293		Air Properties	
T_t	151	424		k	0.02625
T_c	40	313		υ	0.00001655
D_t	0.011			Pr	0.7268
D_c	0.039			β	0.00324675
L	0.65				
Calc		(°C)			
A_t	0.044925				
A_c	0.03982				
$h_{r,t-c}$	0.798473				
$h_{r,c-a}$	5.052819				
Ra	50133.85				
Nu	6.525155				
$h_{c,c-a}$	4.391931				
U	0.032748				
T_c	308.652	35.65204			

TABLE 25. Glass cover temperature calculation 1st iteration

2nd Iteration					
Data		(°C)		Constant	
ε_t	0.07			g	9.81
ε_c	0.8			σ	5.67E-08
T_a	30	303			
T_s	20	293		Air Properties	
T_t	151	424		k	0.02609
T_c	35.65204	308.652		υ	1.64E-05
D_t	0.011			Pr	0.7274
D_c	0.039			β	0.00327
L	0.65				
Calc		(°C)			
A_t	0.044925				
A_c	0.03982				
$h_{r,t-c}$	0.786038				
$h_{r,c-a}$	4.9428				
Ra	29263.83				
Nu	5.696952				
$h_{c,c-a}$	3.811115				
U	0.032064				
T_c	309.0033	36.00331			

TABLE 26. Glass cover temperature calculation 2nd iteration

Heat Transfer				
Energy		Glass Cover		
$\dot{Q}_{t,rad}$	4.06083	τ	0.75	
$\dot{Q}_{c,rad}$	3.080646	γ	0.236	
$\dot{Q}_{c,conv}$	0.857738			
$\dot{Q}_{loss}$	3.938384	Copper tube selective absorber coating		
$\dot{Q}_{gain}$	13.69578	α	0.94	
$\dot{Q}_{total}$	9.757398			
T_{out} (K)	438.0943	G	864.852	
(°C)	165.0943	$\dot{m}$	0.001508	
		C_p	57.2	
		T_{in} (°C)	52	
		(K)	325	

TABLE 27. Calculation of heat transfer and refrigerant output temperature